

UC San Diego

UC San Diego Previously Published Works

Title

Flavor structure of the three-site Higgsless model

Permalink

<https://escholarship.org/uc/item/00m0q4mp>

Journal

Physical Review D - Particles, Fields, Gravitation and Cosmology, 85(3)

ISSN

1550-7998

Authors

Abe, T
Chivukula, RS
Simmons, EH
et al.

Publication Date

2012-02-14

DOI

10.1103/PhysRevD.85.035015

Peer reviewed

The Flavor Structure of the Three-Site Higgsless Model

Tomohiro Abe,¹ R. Sekhar Chivukula,² Elizabeth H. Simmons,² and Masaharu Tanabashi³

¹*Institute of Modern Physics and Center for High Energy Physics, Tsinghua University, Beijing 100084, China*

²*Department of Physics and Astronomy, Michigan State University, East Lansing, MI 48824, USA*

³*Kobayashi-Maskawa Institute for the Origin of Particles and the Universe, Nagoya University, Nagoya 464-8602, Japan
and Department of Physics, Nagoya University, Nagoya 464-8602, Japan*

(Dated: November 6, 2018)

We study the flavor structure of the three-site Higgsless model and evaluate the constraints on the model arising from flavor physics. We find that current data constrain the model to exhibit only minimal flavor violation at tree level. Moreover, at the one-loop level, by studying the leading chiral logarithmic corrections to chirality-preserving $\Delta F = 1$ and $\Delta F = 2$ processes from new physics in the model, we show that the combination of minimal flavor violation and ideal delocalization ensures that these flavor-changing effects are sufficiently small that the model remains phenomenologically viable.

I. INTRODUCTION

Higgsless models [1] of electroweak symmetry breaking provide effective low-energy theories of a strongly-interacting symmetry breaking sector [2, 3]. If the fermions in the model are delocalized (i.e. derive electroweak interactions from multiple gauge groups), Higgsless models can be consistent with electroweak precision measurements [4–10] even at the loop level [11, 12]. The three-site model [11] is the minimal low-energy realization of a Higgsless theory.¹ Its electroweak sector includes only one $SU(2)$ group beyond the usual $SU(2) \times U(1)$ of the standard model, so the gauge spectrum includes only one triplet of the extra vector mesons typically present in such theories; these are the mesons (denoted here by W'^{\pm} and Z') that are analogous to the ρ mesons of QCD. The three-site model retains sufficient complexity, however, to incorporate interesting physics issues related to fermion masses, electroweak observables, and flavor.

As discussed in [11] and reviewed here, the three-site model generically exhibits non-minimal flavor violation (i.e., more than the minimal flavor violation present in the standard model [20, 21]). However, if one assumes that flavor-symmetry breaking enters the Lagrangian only through the delocalization parameters of the right-handed fermions (ϵ_{Rf}), the three-site model then possesses only minimal flavor violation. Moreover, if one also assumes that the (now flavor-universal) delocalization parameter ϵ_L for the left-handed fermions is set to the “ideal” value [10] that correlates the fermion wavefunction with the W -boson wavefunction, then the tree-level electroweak phenomenology of the three-site model agrees completely with that of the standard model.

This situation is modified once loop effects are included. The various parameters in the effective Lagrangian, whether flavor-universal or not, will run, so the conditions of ideal delocalization and minimal flavor violation are not scale-independent. Rather, one may impose these conditions at the scale of the cutoff of the effective three-site theory – the scale of the underlying strong dynamics – and then compute and evaluate corrections to electroweak and flavor observables. In fact, the chiral logarithmic corrections to the flavor-universal electroweak parameters αS and αT [22–25] in the three-site model were computed in references [26–28]; these are the one-loop contributions that dominate in the limit where the masses of the new vector mesons lie far below the cutoff of the effective theory. Likewise, the flavor-dependent corrections to the $Z \rightarrow b\bar{b}$ branching ratio were studied in [12, 29], and the corrections to chirality-non-preserving flavor-dependent process $b \rightarrow s\gamma$ were computed in [30].

This paper completes the investigation of the flavor phenomenology of the three-site model by studying the chiral logarithmic corrections to chirality-preserving flavor-changing processes. We begin by reviewing the essential features of the model and contrasting its flavor structure with that of the standard model. In particular, we establish the conditions under which the three-site model exhibits minimal or non-minimal flavor violation. A brief review (with details in an Appendix) of experimental constraints on flavor-changing effects demonstrates that the tree-level Lagrangian of the three-site model is constrained to a form that, to a good approximation, has only minimal flavor violation; in the rest of the paper, we therefore assume the model exhibits only minimal flavor violation. In section IV, we calculate the corrections to all chirality preserving $\Delta F = 1$ operators that arise from the new physics present in the

¹ This theory is in the same class as models of extended electroweak gauge symmetries [13, 14] motivated by models of hidden local symmetry [15–19]. In particular the three-site model has the same gauge structure as the “BESS” model of [13], but it is the fermion couplings and flavor structure unique to the three-site model [11] that are of particular interest here.

three-site model. We show that, parametrically, the size of the new three-site corrections to $\Delta F = 1$ processes are of the same order as those in the standard model – but that the corrections numerically amount to only a few percent of the standard model contribution. Since no chirality-preserving $\Delta F = 1$ neutral current standard model amplitudes are observable we conclude that, just as in the case of corrections to $Z \rightarrow b\bar{b}$, the additional three-site model chiral logarithmic contributions are not forbidden, and the three-site model remains viable. In section V, we extend our analysis to $\Delta F = 2$ (meson mixing) processes. We find that the combination of ideal delocalization and minimal flavor violation insures that the new contributions to $\Delta F = 2$ box diagrams in the three-site model are smaller than or of order two-loop corrections to these processes in the standard model – and hence are not phenomenologically excluded. The final section of the paper summarizes our conclusions.

II. THE THREE-SITE MODEL

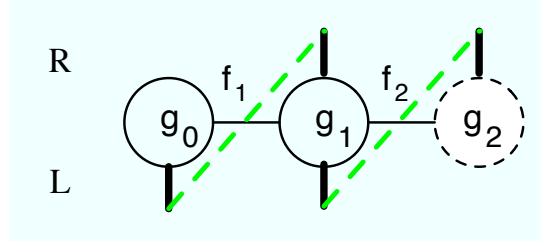


FIG. 1: The three-site model [11], illustrated using “moose” notation [31]. The solid circles represent $SU(2)$ gauge groups, with coupling strengths g_0 and g_1 , and the dashed circle is a $U(1)$ gauge group with coupling g_2 . The horizontal lines represent $SU(2) \times SU(2)/SU(2)$ non-linear sigma model fields, with decay constants $f_{1,2}$, breaking the adjacent global groups down to their diagonal sum. The left-handed fermions, denoted by the lower vertical lines, are located at sites 0 and 1, and the right-handed fermions, denoted by the upper vertical lines, at sites 1 and 2. The dashed green lines correspond to Yukawa couplings, as described in the text. We will denote $g_0 \equiv g$, $g_1 \equiv \tilde{g}$, $g_2 \equiv g'$ and take $g, g' \ll \tilde{g}$.

The three-site $SU(2)_0 \times SU(2)_1 \times U(1)_2$ model [11] is illustrated (using “moose” notation [31]) in Fig. 1 where, as we will see, $SU(2)_0 \times U(1)_2$ is approximately the $SU(2)_L \times U(1)_Y$ of the electroweak interactions, $SU(2)_1$ is a new “hidden” gauge-symmetry [13, 15, 16, 18], and the $U(1)_2$ is embedded as the σ^3 -component of an $SU(2)_2$ global symmetry. We will denote the gauge couplings of the three groups by, $g_0 \equiv g$, $g_1 \equiv \tilde{g}$, and $g_2 \equiv g'$ respectively.² The nonlinear sigma-model and gauge-theory kinetic-energy terms in this model are given by

$$\mathcal{L} = \sum_{i=1,2} \frac{f_i^2}{4} \text{tr} \left(D^\mu \Sigma_i^\dagger D_\mu \Sigma_i \right) - \frac{1}{4} (\vec{W}_0^{\mu\nu})^2 - \frac{1}{4} (\vec{W}_1^{\mu\nu})^2 - \frac{1}{4} B_{\mu\nu}^2, \quad (1)$$

where Σ_1 and Σ_2 are $SU(2) \times SU(2)/SU(2)$ sigma-model fields parameterized by

$$\Sigma_{1,2} = \exp \left(\frac{2i\pi_{1,2}}{f_{1,2}} \right), \quad (2)$$

where $\pi_{1,2} \equiv \pi_{1,2}^a \sigma^a / 2$, and where $\vec{W}_{0,1}^{\mu\nu}$ and $B^{\mu\nu}$ are, respectively, the field-strength tensors of the $SU(2)_{0,1}$ and $U(1)_2$ gauge-groups with corresponding gauge-fields $W_{0,1}^\mu$ and B^μ .

The sigma-model fields transform as

$$\Sigma_1 \rightarrow U_0 \Sigma_1 U_1^\dagger, \quad \Sigma_2 \rightarrow U_1 \Sigma_2 U_2^\dagger, \quad (3)$$

under the $SU(2)_0 \times SU(2)_1 \times SU(2)_2$ global symmetries, and hence the covariant derivatives above are given by

$$D_\mu \Sigma_1 = \partial_\mu \Sigma_1 - ig W_{0\mu}^a \frac{\sigma^a}{2} \Sigma_1 + i\tilde{g} W_{1\mu}^a \Sigma_1 \frac{\sigma^a}{2}, \quad (4)$$

$$D_\mu \Sigma_2 = \partial_\mu \Sigma_2 - i\tilde{g} W_{1\mu}^a \Sigma_2 \frac{\sigma^a}{2} + ig' B_\mu \Sigma_2 \frac{\sigma^3}{2}. \quad (5)$$

² Here g and g' are chosen because, as we will see, these groups are approximately the $SU(2)_W \times U(1)_Y$ of the standard model.

Here $f_{1,2}$ are the f -constants, the analogs of F_π in QCD, associated with the two $SU(2) \times SU(2)/SU(2)$ nonlinear sigma-models, and they satisfy the relation

$$\sqrt{2}G_F = \frac{1}{v^2} = \frac{1}{f_1^2} + \frac{1}{f_2^2} \approx \frac{1}{(250 \text{ GeV})^2} . \quad (6)$$

In [11], for simplicity and to maximize the range of validity of this low-energy effective theory, we took $f_1 = f_2 = \sqrt{2}v$; in this work, in order to identify the origin of various one-loop effects, we will leave $f_{1,2}$ arbitrary, subject to the constraint in Eq. (6) above.

In unitary gauge, $\Sigma_1 = \Sigma_2 \equiv \mathcal{I}$, and the non-linear sigma model kinetic terms yield vector-boson mass matrices. We will work in the limit $g, g' \ll \tilde{g}$, or equivalently

$$x = g/\tilde{g} \ll 1 . \quad (7)$$

We will also define an angle θ

$$\frac{g'}{g} \equiv \frac{\sin \theta}{\cos \theta} , \quad (8)$$

which will equal the usual weak mixing angle up to corrections of order x^2 . In the small x limit, we find the charged-boson masses

$$M_W^2 = \frac{g^2 v^2}{4} + \dots , \quad M_{W'}^2 = \frac{\tilde{g}^2 (f_1^2 + f_2^2)}{4} + \dots , \quad (9)$$

where the mass eigenstates are of the form [13]

$$W_\mu^\pm = W_{0\mu}^\pm + \frac{x f_1^2}{f_1^2 + f_2^2} W_{1\mu}^\pm + \mathcal{O}(x^2) , \quad (10)$$

$$W_\mu^{\prime\pm} = -\frac{x f_1^2}{f_1^2 + f_2^2} W_{0\mu}^\pm + W_{1\mu}^\pm + \mathcal{O}(x^2) . \quad (11)$$

The neutral bosons include a massless photon (A^μ), which corresponds to the eigenvector

$$A_\mu = \frac{e}{g} W_{0\mu}^3 + \frac{e}{\tilde{g}} W_{1\mu}^3 + \frac{e}{g'} B^\mu \quad (12)$$

$$= \sin \theta W_{0\mu}^3 + x \sin \theta W_{1\mu}^3 + \cos \theta B^\mu + \mathcal{O}(x^2) , \quad (13)$$

where e is the electromagnetic coupling

$$\frac{1}{e^2} = \frac{1}{g^2} + \frac{1}{\tilde{g}^2} + \frac{1}{g'^2} . \quad (14)$$

For small x we also have

$$g \approx \frac{e}{\sin \theta} , \quad g' \approx \frac{e}{\cos \theta} . \quad (15)$$

The two other neutral gauge-bosons have masses

$$M_Z^2 = \frac{e^2 v^2}{4 \sin^2 \theta \cos^2 \theta} + \dots , \quad M_{Z'}^2 = \frac{\tilde{g}^2 (f_1^2 + f_2^2)}{4} + \dots , \quad (16)$$

corresponding to the eigenvectors [13]

$$Z_\mu = \cos \theta W_{0\mu}^3 + \frac{x \cos \theta (f_1^2 - f_2^2 \tan^2 \theta)}{f_1^2 + f_2^2} W_{1\mu}^3 - \sin \theta B_\mu + \mathcal{O}(x^2) , \quad (17)$$

$$Z'_\mu = -\frac{x f_1^2}{f_1^2 + f_2^2} W_{0\mu}^3 + W_{1\mu}^3 - \frac{x \tan \theta f_2^2}{f_1^2 + f_2^2} B_\mu + \mathcal{O}(x^2) . \quad (18)$$

As described in [11], working in the limit of small x ($g, g' \ll \tilde{g}$), we get a phenomenologically-acceptable low-energy electroweak model if we identify the light W_μ^\pm and Z_μ with the weak bosons, because the extra states W' and Z' are

much heavier than ordinary electroweak gauge bosons ($M_{W,Z}^2 \ll M_{W',Z'}^2$). In particular (after including ideal fermion delocalization [10]) all tree-level standard model predictions are reproduced up to corrections of order x^4 . Note also that, in the limit $f_1 \rightarrow \infty$ for fixed v , the gauge boson mass eigenstates of the three-site model reduce³ to those of the standard model with the identification of $SU(2)_0 \times U(1)_2$ with $SU(2)_L \times U(1)_Y$.

The three-site model also incorporates the ordinary quarks and leptons, and requires the presence of additional heavy vectorial $SU(2)_1$ fermions that mirror the light fermions. These heavy Dirac fermions are the analogs of the lowest Kaluza-Klein (KK) fermion modes which would be present in an extra-dimensional theory. The quark “Yukawa” sector of the three-site model illustrated in Fig. 1 is:

$$\mathcal{L}_{mass} = -\bar{q}_L^{(0)} \Sigma_1 \mathfrak{m}_1 q_R^{(1)} - \bar{q}_L^{(1)} \mathbb{M} q_R^{(1)} - \bar{q}_L^{(1)} \Sigma_2 \begin{pmatrix} \mathfrak{m}_{2u} & 0 \\ 0 & \mathfrak{m}_{2d} \end{pmatrix} \begin{pmatrix} u_R^{(2)} \\ d_R^{(2)} \end{pmatrix} + h.c. , \quad (19)$$

where the quark fields $q_L^{(0)}$, $q_{L,R}^{(1)}$, $u_R^{(2)}$, and $d_R^{(2)}$ are three-component vectors in flavor space, \mathfrak{m}_1 , \mathbb{M} , and $\mathfrak{m}_{2u,2d}$ are 3×3 matrices in flavor space, and the summation over flavor and gauge indices is implicit. The transformation properties of the quarks under the global $SU(2)_0 \times SU(2)_1 \times SU(2)_2$ symmetries are given by

$$q_L^{(0)} \rightarrow U_0 q_L^{(0)} , \quad (20)$$

$$q_{R,L}^{(1)} \rightarrow U_1 q_{R,L}^{(1)} , \quad (21)$$

$$\begin{pmatrix} u_R^{(2)} \\ d_R^{(2)} \end{pmatrix} \rightarrow U_2 \begin{pmatrix} u_R^{(2)} \\ d_R^{(2)} \end{pmatrix} . \quad (22)$$

The $SU(2)_0 \times SU(2)_1$ properties of the quarks follow from the assignments above; the hypercharge properties are fixed by insuring the correct values of the electric charges, and hence under $U(1)_2$ we require that the $q_L^{(0)}$ and $q_{L,R}^{(1)}$ fields carry charge 1/6, while the $u_R^{(2)}$ and $d_R^{(2)}$ carry charges +2/3 and −1/3 respectively.

We will work in the limit where the eigenvalues⁴ of \mathbb{M} are much greater than those for \mathfrak{m}_1 and $\mathfrak{m}_{2u,d}$ and where the heavy fermions are essentially the $q^{(1)}$ doublets with mass-squareds given approximately by the eigenvalues of $\mathbb{M}\mathbb{M}^\dagger$. In this limit the matrix $\epsilon_L \equiv \mathfrak{m}_1 \cdot \mathbb{M}^{-1}$ controls the “delocalization” of the left-handed fermions, *i.e.* the degree to which the light left-handed mass eigenstate fields are admixtures of fermions at the first two sites. In [11], it was assumed that \mathbb{M} and \mathfrak{m}_1 were flavor-diagonal, so that ϵ_L was likewise proportional to the identity in flavor-space. Furthermore, it was shown that the proportionality constant could be adjusted (a process called “ideal fermion delocalization”) to eliminate potentially dangerous tree-level contributions to the electroweak parameter αS [4–10]. In this work, we confirm that the precision electroweak and flavor data directly constrain ϵ_L to be flavor universal and close to the ideal delocalization form. Therefore we will take ϵ_L to be flavor-universal, at tree-level in the three-site model, so that all of the flavor-breaking is encoded in the values of Yukawa couplings to the right-handed fermions. As we show below, in this limit the three-site model at tree-level has precisely the same flavor structure as the standard model: all of the tree-level couplings of the left-handed fermions to the gauge bosons are flavor-diagonal and equal, and flavor-changing neutral currents are suppressed [11].

Limits on the WWZ coupling imply that the W' and Z' bosons must be heavier than about 400 GeV, while limits on the unitarity of $W_L W_L$ scattering show they must be lighter than about 1 TeV [10]. On the other hand, limits on αT imply that the heavy fermions must have masses greater than about 2 TeV [11].

III. FLAVOR SYMMETRIES AND STRUCTURE

In this section we consider the tree-level flavor structure of the three-site model. We begin with a review of the flavor symmetries of the standard model and generalize to the three-site model. Then, we consider the effective Lagrangian that results from “integrating out” the heavy fermions and analyze the tree-level gauge-couplings.

³ While the particular expressions for the W and Z mass eigenstates in Eqs. (10) and (17) were calculated perturbatively for $x \ll 1$, the reduction of the extended electroweak gauge to its standard model counterpart in the $f_1 \rightarrow \infty$ limit (with fixed v) is a more general result that follows directly from the decoupling theorem [32].

⁴ More properly, the eigenvalues of $\mathbb{M}\mathbb{M}^\dagger$ are much greater than those of $\mathfrak{m}_1 \mathfrak{m}_1^\dagger$ or $\mathfrak{m}_{2u,d} \mathfrak{m}_{2u,d}^\dagger$.

A. GIM Flavor Symmetries of the standard model

Before proceeding to discuss the flavor structure of the three-site model in detail, we first briefly review the flavor structure of the Yukawa sector of the standard model

$$\mathcal{L}_{Yuk} = -\bar{q}_{Li}\lambda_d^{ij}\varphi d_{Rj} - \bar{q}_{Li}\lambda_u^{ij}\tilde{\varphi}u_{Rj} + h.c. \quad (23)$$

Here the q_{Li} , u_{Rj} , and d_{Rj} fields are the three flavors of left-handed quarks, and right-handed up- and down-type quarks respectively, i and j are flavor indices, and $\lambda_{d,u}^{ij}$ are the Yukawa-coupling matrices for down- and up-quarks.

In the standard model, these Yukawa terms are the only interactions that distinguish among flavors. The gauge interactions respect an $SU(3)_L \times SU(3)_{uR} \times SU(3)_{dR}$ global symmetry. The Yukawa couplings $\lambda_{u,d}$ can then be treated as “spurions”, and they can be classified by their transformation properties under these symmetries [20]. In particular, the standard model would be invariant under an arbitrary global flavor symmetry transformation *if* the Yukawa couplings transformed as follows

$$\lambda_u \rightarrow L\lambda_u R_u^\dagger \quad \lambda_d \rightarrow L\lambda_d R_d^\dagger, \quad (24)$$

so that $\lambda_{u,d}$ transformed, respectively, as elements of the $(3, \bar{3}, 1)$ and $(3, 1, \bar{3})$ representations under $SU(3)_L \times SU(3)_{uR} \times SU(3)_{dR}$.

The $SU(3)_L \times SU(3)_{uR} \times SU(3)_{dR}$ symmetries are sufficient to diagonalize *either* λ_u or λ_d . Therefore, there can be no tree-level flavor-changing neutral currents: we can always choose to work in a basis in which λ_d (for example) is diagonal, and in this basis the Z -boson will not connect quarks from different generations. In other words, the $SU(3)_L \times SU(3)_{uR} \times SU(3)_{dR}$ global symmetry underlies the GIM mechanism [33]. The same, of course, is *not* true of the charged weak currents: the mismatch in the L transformations required to diagonalize the λ_u and λ_d couplings results in the CKM matrix [34, 35]. In addition, to the extent that the $\lambda_{u,d}$ are *small* parameters, flavor-violating effects are suppressed by various powers of these couplings. The flavor transformation properties of the amplitudes that give rise to these flavor-violating effects can be used to understand the structure and order of magnitude of the leading standard model contributions.⁵

The same reasoning can be extended beyond the standard model as well: by classifying the flavor-transformation properties of the new interactions, one can understand the structure and order of magnitude of flavor-violating processes in these new theories. From a symmetry point of view, the *minimal* amount of flavor violation in any theory is that which exists in the standard model [20]. In particular, the quark sector of any theory must include “spurions” that transform as $(3, \bar{3}, 1)$ and $(3, 1, \bar{3})$ under $SU(3)_L \times SU(3)_{uR} \times SU(3)_{dR}$ to account for the observed quark masses. This idea has been termed “Minimal Flavor Violation” [21]. Any new interactions in the model should, otherwise, be as flavor-symmetric as possible in order to avoid generating large flavor-changing neutral currents.

B. Flavor Structure of the Three-Site Model at Tree Level

We now examine the flavor structure of the three-site model. We begin by defining the global symmetry group $SU(3)_L \times SU(3)_{LD} \times SU(3)_{RD} \times SU(3)_{uR} \times SU(3)_{dR}$ under which the fields transform as:

$$\begin{aligned} q_L^{(0)} &\rightarrow L \cdot q_L^{(0)} \\ q_L^{(1)} &\rightarrow L_D \cdot q_L^{(1)} \\ q_R^{(1)} &\rightarrow R_D \cdot q_R^{(1)} \\ u_R^{(2)} &\rightarrow R_u \cdot u_R^{(2)} \\ d_R^{(2)} &\rightarrow R_d \cdot d_R^{(2)}, \end{aligned} \quad (25)$$

where L , L_D , R_D , R_u , and R_d are arbitrary elements of $SU(3)_L$, $SU(3)_{LD}$, $SU(3)_{RD}$, $SU(3)_{uR}$, and $SU(3)_{dR}$ respectively. These symmetries are broken by the interactions in Eq. (19), and the various masses are “spurions” – in

⁵ One subtlety in this type of reasoning is worth emphasizing: sometimes, in cases that correspond to “long-distance” effects, some of the dependence on the quark masses is non-analytic. This explains, for example, why the “box diagram” contributions to $\Delta S = 2$ processes in the standard model appear to be suppressed only by *two* powers of quark masses instead of the four powers one would expect on the basis of flavor symmetries – two powers of quark mass appear in the denominator after loop integration, canceling two in the numerator that are there due to the flavor and chiral structure.

particular, the theory would be invariant under $SU(3)_L \times SU(3)_{LD} \times SU(3)_{RD} \times SU(3)_{uR} \times SU(3)_{dR}$ transformations if the mass-parameters were simultaneously changed as follows:

$$\begin{aligned}\mathfrak{m}_1 &\rightarrow L \cdot \mathfrak{m}_1 \cdot R_D^\dagger \\ \mathbf{M} &\rightarrow L_D \cdot \mathbf{M} \cdot R_D^\dagger \\ \mathfrak{m}_{2u} &\rightarrow L_D \cdot \mathfrak{m}_{2u} \cdot R_u^\dagger \\ \mathfrak{m}_{2d} &\rightarrow L_D \cdot \mathfrak{m}_{2d} \cdot R_d^\dagger.\end{aligned}\tag{26}$$

Of course the mass matrices in Eq. (19) are fixed, and do not transform – so their presence breaks the flavor symmetries. In general, without any further assumptions about the structure of these masses, one could go to a basis where \mathfrak{m}_1 and either \mathfrak{m}_{2u} or \mathfrak{m}_{2d} are diagonal – but one would not have freedom to diagonalize either \mathfrak{m}_2 or \mathbf{M} . This shows, as expected, that without further assumptions about the masses the three-site model has non-minimal flavor violation.

Combining the left- and right-handed quarks into twelve-component vectors (suppressing flavor indices)

$$\mathcal{Q}_L = \begin{pmatrix} q_L^{(0)} = \begin{pmatrix} u_L^{(0)} \\ d_L^{(0)} \end{pmatrix} \\ q_L^{(1)} = \begin{pmatrix} u_L^{(1)} \\ d_L^{(1)} \end{pmatrix} \end{pmatrix}, \quad \mathcal{Q}_R = \begin{pmatrix} q_R^{(2)} = \begin{pmatrix} u_R^{(2)} \\ d_R^{(2)} \end{pmatrix} \\ q_R^{(1)} = \begin{pmatrix} u_R^{(1)} \\ d_R^{(1)} \end{pmatrix} \end{pmatrix},\tag{27}$$

the 12×12 mass matrix for the quark sector may be written (each block is 6×6)

$$\mathcal{M} = \begin{pmatrix} 0 & \Sigma_1 \otimes \mathfrak{m}_1 \\ \Sigma_2 \otimes \begin{pmatrix} \mathfrak{m}_{2u} & 0 \\ 0 & \mathfrak{m}_{2d} \end{pmatrix} & \mathcal{I}_{2 \times 2} \otimes \mathbf{M} \end{pmatrix},\tag{28}$$

where we include the factors of $\Sigma_{1,2}$ so as to maintain the $SU(2)_0 \times SU(2)_1 \times SU(2)_2$ global symmetry and, hence, an $SU(2)_0 \times SU(2)_1 \times U(1)_2$ gauge invariance. In the limit in which the eigenvalues of \mathbf{M} are larger than those of \mathfrak{m}_1 , \mathfrak{m}_{2u} , or \mathfrak{m}_{2d} , this matrix has the usual “seesaw” form. It is convenient to define the 3×3 flavor-space matrices

$$\epsilon_L = \mathfrak{m}_1 \cdot \mathbf{M}^{-1} \rightarrow L \cdot \epsilon_L \cdot L_D^\dagger,\tag{29}$$

$$\epsilon_{Ru} = \mathfrak{m}_{2u}^\dagger \cdot (\mathbf{M}^\dagger)^{-1} \rightarrow R_u \cdot \epsilon_{Ru} \cdot R_D^\dagger,\tag{30}$$

$$\epsilon_{Rd} = \mathfrak{m}_{2d}^\dagger \cdot (\mathbf{M}^\dagger)^{-1} \rightarrow R_d \cdot \epsilon_{Rd} \cdot R_D^\dagger,\tag{31}$$

which, from Eq. (25), have the flavor transformation properties indicated. The elements of these matrices are, in the seesaw limit, small quantities. Diagonalizing $\mathcal{M}\mathcal{M}^\dagger$ and $\mathcal{M}^\dagger\mathcal{M}$, we find the light and heavy mass eigenstate fields q and Q , whose components are approximately related to the gauge-eigenstate fields by⁶

$$q_L^{(0)} \simeq -q_L + \Sigma_1 \epsilon_L Q_L\tag{32}$$

$$q_L^{(1)} \simeq Q_L + \epsilon_L^\dagger \Sigma_1^\dagger q_L,\tag{33}$$

and

$$q_R^{(2)} \simeq q_R + \begin{pmatrix} \epsilon_{Ru} & 0 \\ 0 & \epsilon_{Rd} \end{pmatrix} \Sigma_2^\dagger Q_R\tag{34}$$

$$q_R^{(1)} \simeq Q_R - \Sigma_2 \begin{pmatrix} \epsilon_{Ru}^\dagger & 0 \\ 0 & \epsilon_{Rd}^\dagger \end{pmatrix} q_R.\tag{35}$$

Here, for convenience, we have chosen fields q_L , q_R , and $Q_{L,R}$ to transform under the $SU(2)_0$, $SU(2)_2$, and $SU(2)_1$ global symmetry groups respectively.

⁶ The sign convention of the fields was chosen to agree with [11].

To investigate flavor phenomenology in the three-site model we may “integrate out” the heavy Dirac Fermions Q at tree-level. Keeping terms with two factors of the small ϵ matrices, this corresponds to inserting Eqs. (32) - (35) into the fermion three-site model Lagrangian, and setting the heavy fields $Q \equiv 0$. Doing so, we obtain:

$$\begin{aligned} \mathcal{L}_{eff} = & \bar{q}_L i \not{D} q_L + \bar{u}_R i \not{D} u_R + \bar{d}_R i \not{D} d_R - \left[\bar{q}_L \epsilon_L \Sigma_1 \Sigma_2 \mathbb{M} \begin{pmatrix} \epsilon_{Ru}^\dagger & 0 \\ 0 & \epsilon_{Rd}^\dagger \end{pmatrix} \begin{pmatrix} u_R \\ d_R \end{pmatrix} + h.c. \right] \\ & + \bar{q}_L \epsilon_L \left[\gamma^\mu \Sigma_1 (i D_\mu \Sigma_1^\dagger) \right] \epsilon_L^\dagger q_L + \bar{q}_R \begin{pmatrix} \epsilon_{Ru} & 0 \\ 0 & \epsilon_{Rd} \end{pmatrix} \left[\gamma^\mu \Sigma_2^\dagger (i D_\mu \Sigma_2) \right] \begin{pmatrix} \epsilon_{Ru}^\dagger & 0 \\ 0 & \epsilon_{Rd}^\dagger \end{pmatrix} q_R . \end{aligned} \quad (36)$$

Here we have neglected terms that result purely in wavefunction renormalization of the fermion fields, and terms of $\mathcal{O}(\epsilon^3)$. An important check on this result is that all of the terms in Eq. (36) are invariant under an arbitrary $SU(3)_L \times SU(3)_{LD} \times SU(3)_{RD} \times SU(3)_{uR} \times SU(3)_{dR}$ transformation, Eq. (25), *combined with* the spurion parameter change in Eq. (26). We emphasize that Eq. (36) is entirely basis independent – and therefore any results derived from it are parameterization and phase independent as well.

The last term on the first line of Eq. (36) yields the up- and down-quark masses

$$\mathcal{M}_u = \epsilon_L \mathbb{M} \epsilon_{Ru}^\dagger \rightarrow L \cdot \mathcal{M}_u \cdot R_u^\dagger \quad (37)$$

$$\mathcal{M}_d = \epsilon_L \mathbb{M} \epsilon_{Rd}^\dagger \rightarrow L \cdot \mathcal{M}_d \cdot R_d^\dagger , \quad (38)$$

which transform precisely as the Yukawa couplings in the standard model, Eq. (24). Without loss of generality, we may write the most general quark mass matrices as

$$\mathcal{M}_u = \Lambda_u \Delta_u P_u^\dagger , \quad (39)$$

for up-quarks, and

$$\mathcal{M}_d = \Lambda_d \Delta_d P_d^\dagger , \quad (40)$$

for down-quarks. Here $\Delta_{u,d}$ are the diagonal up- and down-quark mass matrices, with all masses positive, and $\Lambda_{u,d}$ and $P_{u,d}$ are arbitrary unitary matrices.⁷ Just as in the standard model the $SU(3)_L \times SU(3)_{uR} \times SU(3)_{dR}$ subgroup of the three-site flavor symmetry group is sufficient to diagonalize either the mass matrix of the up- or down-type quarks, but not both simultaneously. In a basis in which the down-quark masses are diagonal, from Eq. (26), we have

$$\mathcal{M}_d = \Delta_d \quad (41)$$

$$\mathcal{M}_u = (\Lambda_d^\dagger \Lambda_u) \Delta_u \equiv V_{CKM}^\dagger \Delta_u , \quad (42)$$

where V_{CKM} is the usual quark-mixing matrix. Note also that the field $\Sigma_1 \Sigma_2$ in the last term of the first line of Eq. (36) contains precisely the unphysical Goldstone boson π_W corresponding to the light W gauge-boson.

The presence of the additional terms in the second line of Eq. (36), involving ϵ_L , ϵ_{Ru} , and ϵ_{Rd} , implies that the three-site model generically includes non-minimal flavor violation. To minimize the amount of flavor violation in the model, as discussed in [11], we will assume⁸ that both \mathfrak{m}_1 and \mathbb{M} are *flavor-universal*, and proportional to the identity matrix

$$\mathbb{M} \equiv M \cdot \mathcal{I}_{3 \times 3} , \quad (43)$$

$$\mathfrak{m}_1 \equiv m_1 \cdot \mathcal{I}_{3 \times 3} , \quad (44)$$

except where explicitly stated otherwise. If $\mathfrak{m}_1, \mathbb{M} \propto \mathcal{I}_{3 \times 3}$ then, from Eqs. (29 – 31) and in the basis in which \mathcal{M}_d is diagonal,

$$\epsilon_L \propto \mathcal{I} , \quad (45)$$

$$\epsilon_{Ru} \propto V_{CKM}^\dagger \Delta_u , \quad (46)$$

$$\epsilon_{Rd} \propto \Delta_d . \quad (47)$$

⁷ Here and throughout this note we assume the freedom to make arbitrary phase redefinitions of the quark fields. In principle, due to the axial anomaly, these redefinitions will be accompanied by a change in the QCD $\bar{\theta}$ parameter.

⁸ This situation is similar to the assumed flavor-universality of soft SUSY breaking masses in supersymmetric extensions of the standard model.

Here we see explicitly that all flavor-violation is precisely of a form determined by the quark-mass matrices, as expected in a minimally flavor-violating theory. This assumption is also directly supported by constraints from precision electroweak data, and data on flavor violation in the charged-lepton and quark sectors, as we will summarize in section III D and explain in the Appendix.

C. Gauge-Boson Couplings at Tree-Level

The light quark fields q_L , u_R and d_R in the effective Lagrangian of Eq. (36) couple only to the $SU(2)_0 \times U(1)_2$ gauge-eigenstate fields

$$D_\mu q_L = \left[\partial_\mu - igW_{0\mu}^a \frac{\sigma^a}{2} - ig' \frac{B_\mu}{6} \right] q_L, \quad (48)$$

$$D_\mu \begin{pmatrix} u_R \\ d_R \end{pmatrix} = \left[\partial_\mu - ig' B_\mu \begin{pmatrix} \frac{2}{3} & 0 \\ 0 & -\frac{1}{3} \end{pmatrix} \right] \begin{pmatrix} u_R \\ d_R \end{pmatrix}. \quad (49)$$

Using Eqs. (10 – 11) and (17 – 18), the fermion kinetic energy terms give the conventional couplings of the light W and Z bosons to the quarks. From Eqs. (41 – 42), we see that these interactions have the same flavor structure as in the standard model. The fermion kinetic energy terms also give rise to couplings of the light quarks to the heavy gauge bosons

$$- \frac{g}{\sqrt{2}} \frac{x f_1^2}{f_1^2 + f_2^2} W'_\mu{}^\pm \sigma^\pm - \left(\frac{g x f_1^2}{f_1^2 + f_2^2} \frac{\sigma^3}{2} + \frac{g' x f_2^2}{f_1^2 + f_2^2} Y \right) Z'_\mu + \mathcal{O}(x^2), \quad (50)$$

where the $\sigma^{\pm,3}$ and Y encode the $SU(2) \times U(1)_Y$ quantum numbers of the quark. As expected for minimal flavor violation, there are no tree-level flavor-changing neutral currents and the charged-current flavor structure is determined by the CKM mixing matrix.

In addition, the terms on the second line Eq. (36) give rise to additional tree-level couplings to the gauge-bosons. In unitary gauge, we see that these terms give rise to terms involving the neutral and charged gauge-bosons

$$\epsilon_L \Sigma_1 (i D_\mu \Sigma_1^\dagger) \epsilon_L^\dagger \rightarrow (-gW_{0\mu}^a + \tilde{g}W_{1\mu}^a) \frac{\sigma^a}{2} \epsilon_L \epsilon_L^\dagger = \begin{cases} \left(-\frac{g}{\sqrt{2}} \frac{f_2^2}{f_1^2 + f_2^2} W_\mu^\pm + \frac{\tilde{g}}{\sqrt{2}} W'_\mu{}^\pm \right) \sigma^\pm \epsilon_L \epsilon_L^\dagger, & a = \pm \\ \left(-g \frac{f_2^2}{\cos \theta (f_1^2 + f_2^2)} Z_\mu + \tilde{g} Z'_\mu \right) \frac{\sigma^3}{2} \epsilon_L \epsilon_L^\dagger, & a = 3 \end{cases}, \quad (51)$$

$$\epsilon_R \Sigma_2^\dagger (i D_\mu \Sigma_2) \epsilon_R^\dagger \rightarrow \epsilon_R \left(\tilde{g} W_{1\mu}^a \frac{\sigma^a}{2} - g' B_\mu \frac{\sigma^3}{2} \right) \epsilon_R^\dagger = \begin{cases} \left(\frac{g}{\sqrt{2}} \frac{f_1^2}{f_1^2 + f_2^2} W_\mu^\pm + \frac{\tilde{g}}{\sqrt{2}} W'_\mu{}^\pm \right) \epsilon_R \sigma^\pm \epsilon_R^\dagger, & a = \pm \\ \left(g \frac{f_1^2}{\cos \theta (f_1^2 + f_2^2)} Z_\mu + \tilde{g} Z'_\mu \right) \epsilon_R \frac{\sigma^3}{2} \epsilon_R^\dagger, & a = 3 \end{cases}, \quad (52)$$

where, for convenience, we have defined

$$\epsilon_R \equiv \begin{pmatrix} \epsilon_{Ru} & 0 \\ 0 & \epsilon_{Rd} \end{pmatrix}. \quad (53)$$

Using Eqs. (45 – 47) we again see that there are no flavor-changing neutral currents at tree-level, and that the strengths of charged-current processes are proportional to the CKM matrix. Comparing Eqs. (51) and (48), we see that the light-fermion portions of the $SU(2)$ currents to which the W and Z bosons couple are

$$j_L^{a\mu} \supset \bar{q}_L \gamma^\mu \frac{\sigma^a}{2} \left(1 - \frac{\epsilon_L \epsilon_L^\dagger f_2^2}{f_1^2 + f_2^2} \right) q_L, \quad (54)$$

consistent with equation (27) of [29].⁹

Combining the terms in Eq. (51) with those in Eq. (50), we see that the W' couplings to light fermions are proportional to

$$\tilde{g} \epsilon_L \epsilon_L^\dagger - \frac{g x f_1^2}{f_1^2 + f_2^2}. \quad (55)$$

⁹ Note here, again, that in the limit $f_1 \rightarrow \infty$ and with v fixed the three-site model reduces to the standard model – in this case for the light fermion couplings as well.

Hence, if ϵ_L is flavor-universal and satisfies

$$\epsilon_L \epsilon_L^\dagger = \frac{x^2 f_1^2}{f_1^2 + f_2^2} \cdot \mathcal{I} + \mathcal{O}(x^4) \quad (56)$$

$$= \frac{f_1^2}{v^2} \frac{M_W^2}{M_{W'}^2} \cdot \mathcal{I} + \mathcal{O}(x^4), \quad (57)$$

the couplings of the light fermions to the W'_μ *vanish*, along with the T^3 coupling of the Z'_μ . Defining

$$(\epsilon_L^{ideal})^2 = \frac{x^2 f_1^2}{f_1^2 + f_2^2} = \frac{f_1^2}{v^2} \frac{M_W^2}{M_{W'}^2}, \quad (58)$$

we see that $\epsilon_L^\dagger \epsilon_L = (\epsilon_L^{ideal})^2 \cdot \mathcal{I}$ is equivalent to the “ideal fermion delocalization” condition of ref. [10]. As we demonstrate in the Appendix, this amount of delocalization insures the equality of the tree-level three-site model couplings to those of the standard model, up to corrections of order x^4 [10] and the absence of large tree-level corrections to precision electroweak measurements [4–11]. The terms in equation (52) can, however, yield small, and potentially flavor-dependent, *right-handed* [8, 11] W -couplings proportional to the product of the masses of the quarks involved.

D. Experimental constraints on ϵ_L

As stated earlier, assuming ϵ_L is proportional to the identity matrix minimizes the amount of flavor violation in the model and assuming the proportionality constant comes from equation (57) minimizes the size of precision electroweak corrections. Here, we note that precision electroweak measurements and bounds on flavor-violation in the charged-lepton and quark sectors specifically constrain ϵ_L to take this same “ideal delocalization” form.

Starting with the quark sector, we adopt the basis in which the down-quark mass matrix is diagonal. Then the elements of $(\epsilon_L \epsilon_L^\dagger) \equiv \eta$ potentially induce flavor-dependent Z and Z' couplings to quarks. In other words, we are interested in the degree to which experiment allows this matrix to depart from the form in equation (57), where each diagonal element has the value $(\epsilon_L^{ideal})^2 = \frac{f_1^2}{v^2} \frac{M_W^2}{M_{W'}^2}$ and the off-diagonal elements simply vanish. As detailed in the Appendix, data on flavor-changing neutral currents in the B-meson, Kaon, and D-meson systems and Z -pole measurements of the rate at which the Z decays to heavy quarks, as opposed to all hadrons, require at 90%CL that (here we bound the absolute value of each matrix element)

$$|\eta - (\epsilon_L^{ideal})^2 \cdot \mathcal{I}| \lesssim (\epsilon_L^{ideal})^2 \left(\frac{M_{W'}}{400 \text{ GeV}} \right)^2 \begin{pmatrix} 0.30 & 0.0060 \frac{\sqrt{2}v}{f_1} & 0.0285 \frac{\sqrt{2}v}{f_1} \\ 0.0060 \frac{\sqrt{2}v}{f_1} & 0.30 & 0.202 \frac{\sqrt{2}v}{f_1} \\ 0.0285 \frac{\sqrt{2}v}{f_1} & 0.202 \frac{\sqrt{2}v}{f_1} & 0.09 \end{pmatrix}, \quad (59)$$

subject to the further constraint that the first two diagonal elements must be nearly identical

$$|\eta_{11} - \eta_{22}| \leq 2.61 \times 10^{-3} \left(\frac{f_1}{\sqrt{2}v} \right) = 0.0323 (\epsilon_L^{ideal})^2 \left(\frac{M_{W'}}{400 \text{ GeV}} \right)^2 \left(\frac{\sqrt{2}v}{f_1} \right). \quad (60)$$

In other words, experiment essentially constrains η to be of the form shown in (57).

Analogously, in the charged-lepton sector, we adopt the basis in which the charged lepton mass matrix is diagonal and ignore neutrino masses. Then the elements of $(\epsilon_L \epsilon_L^\dagger)_{lepton} \equiv \eta_\ell$ potentially induce flavor-dependent Z and Z' couplings to the charged leptons. Again, we are interested in the degree to which experiment allows this matrix to depart from the form in equation (57). LEPEWWG bounds on the Z boson’s decay rates into charged leptons and on Z -pole leptonic charge asymmetries, as well as searches for the flavor-violating decays $\mu \rightarrow 3e$, $\tau \rightarrow e\mu\mu$ and $\tau \rightarrow \mu ee$, combine to require at 90%CL that (again, we bound the absolute value of each matrix element)

$$|\eta_\ell - (\epsilon_L^{ideal})^2 \cdot \mathcal{I}| \lesssim (\epsilon_L^{ideal})^2 \left(\frac{M_{W'}}{400 \text{ GeV}} \right)^2 \begin{pmatrix} 0.036 & 0.00013 & 0.034 \\ 0.00013 & 0.075 & 0.036 \\ 0.034 & 0.036 & 0.12 \end{pmatrix} \quad (61)$$

so that the matrix must have the form of (57). Again, details are given in the Appendix.

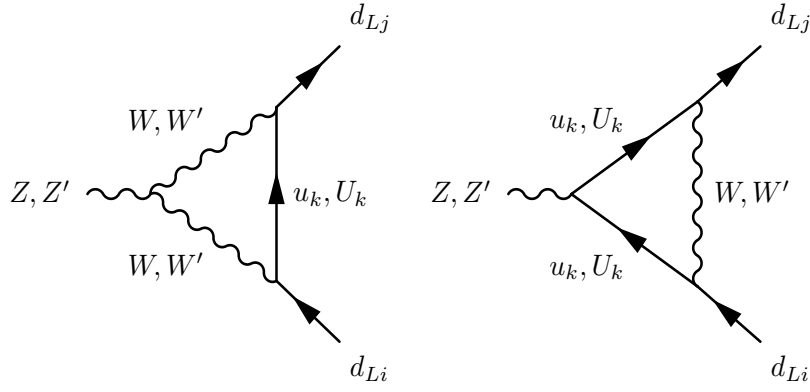


FIG. 2: Vertex diagrams contributing to the processes $Z \rightarrow d_i \bar{d}_j$ and $Z' \rightarrow d_i \bar{d}_j$. Each diagram is summed over the internal u_k and U_k flavors. Due to ideal delocalization, the vertices connecting the heavy W' boson to light $u\bar{d}$ quark pairs are absent.

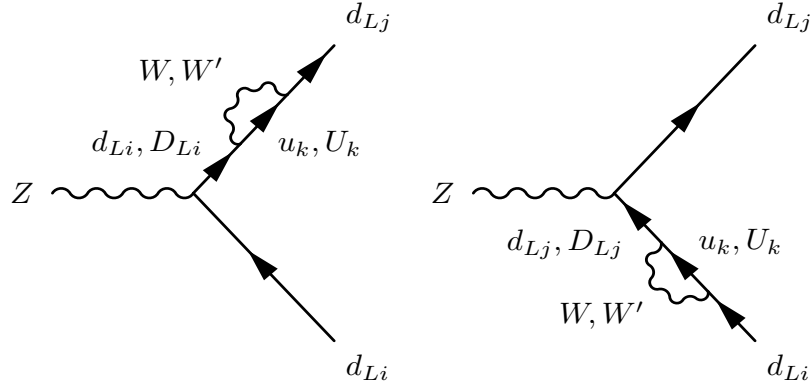


FIG. 3: Wavefunction renormalization diagrams which must be included in the $Z \rightarrow d_i \bar{d}_j$ computation. The analogous Z' contributions are suppressed, relative to the leading vertex contributions.

IV. $\Delta F = 1$ PROCESSES AT ONE LOOP

If \mathfrak{m}_1 and \mathfrak{M} are assumed to be flavor-diagonal and the ratio ϵ_L is chosen to yield ideal delocalization, then tree-level three-site model electroweak phenomenology agrees with the standard model. The situation is modified at the loop level, however. The effective Lagrangian parameters \mathfrak{m}_1 , \mathfrak{M} , and $\mathfrak{m}_{2u,2d}$ run in the usual way, and therefore the conditions of ideal delocalization and minimal flavor violation are not scale-independent. Rather, we may impose these conditions at the scale of the cutoff Λ of the effective three-site theory and then compute the chiral-logarithmic corrections to observables at accessible energy scales.

In this section, we consider the three-site corrections to all chirality preserving $\Delta F = 1$ operators, and review the results of [30] on the chirality non-preserving process $b \rightarrow s\gamma$. We show that, parametrically, the sizes of the new three-site corrections to $\Delta F = 1$ processes are of the same order as those in the standard model – but that the corrections numerically amount to only a few % of the standard model contribution. We conclude that, just as in the case of corrections to $Z \rightarrow b\bar{b}$, the additional three-site model chiral logarithmic contributions are not forbidden, and the three-site model is consistent with data. In the next section we extend our analysis to $\Delta F = 2$ (meson mixing) processes.

A. $Z \rightarrow \bar{f}f'$

We begin with the calculation of the new contributions to the process $Z \rightarrow \bar{f}f'$ in the three-site model. All contributions in the three-site model are shown in Fig. 2, though those involving only light particles (*i.e.*, those not involving either the heavy W' or Z' gauge bosons, or the heavy quarks) just reproduce the standard model results. In addition, one must properly account for the wavefunction corrections illustrated in Fig. 3. We have performed these calculations in 't-Hooft-Feynman gauge in the three-site model (the appropriate Feynman rules can be extracted from

references [27, 30]), but the result is easily understood in terms of the effective Lagrangian/renormalization group calculation of the flavor non-universal contributions to the $Z \rightarrow b\bar{b}$ branching ratio discussed in [29].

Applying the results of [29], we see that the dominant one-loop effect in $Z \rightarrow \bar{f}f'$ is the flavor-dependent running of the effective Lagrangian parameter \mathcal{M} from the cutoff, Λ (where ideal delocalization and minimal flavor violation are imposed on the effective Lagrangian parameters) to the scale of the heavy fermion masses. This effect is due to wavefunction renormalization of the site-1 fermion fields $q_L^{(1)}$, Fig. 4. Generalizing the calculations of [29], this wavefunction renormalization results in the running of the parameter $\epsilon_L \epsilon_L^\dagger$

$$\mu \frac{d}{d\mu} (\epsilon_L \epsilon_L^\dagger) = - \frac{2}{(4\pi)^2 f_2^2} [\mathcal{M}_u \mathcal{M}_u^\dagger + \mathcal{M}_d \mathcal{M}_d^\dagger] , \quad (62)$$

where $\mathcal{M}_{u,d}$ are the mass matrices of the light up- and down-quarks. We see that the flavor transformation properties (Eq. (26)) of the left- and right-hand sides of this equation match. Note also that the (dominant) contribution illustrated in Fig. 4 arises from the unphysical Nambu-Goldstone boson, π_2 , of Eq. (2), whose couplings are proportional to the flavor-dependent parameters $\mathfrak{m}_{2u,2d}$ and inversely proportional to f_2 .

Below the scale of the heavy quark masses, this running ceases. Furthermore, there is a cancellation between the vertex and wavefunction diagrams of Figs. 2 and 3 because the $SU(2)_0$ global symmetry to which the Z is largely coupled, is conserved (up to corrections suppressed by electroweak couplings). Denoting the scale of the heavy fermion masses by M , *c.f.* Eq. (43), we see that the chiral-logarithmic correction to the parameter $\epsilon_L \epsilon_L^\dagger$ is given by

$$\Delta(\epsilon_L \epsilon_L^\dagger) = \frac{1}{(4\pi)^2 f_2^2} [\mathcal{M}_u \mathcal{M}_u^\dagger + \mathcal{M}_d \mathcal{M}_d^\dagger] \log \frac{\Lambda^2}{M^2} . \quad (63)$$

As usual, from Eqs. (41 – 42), the first term gives rise to flavor-changing *down* quark couplings while the second to flavor-changing *up* quark couplings. In the case of s and d quarks, for example, from Eq. (54) we see that the running from the cutoff Λ to the scale M of the heavy quark masses yields the flavor-changing Z -boson coupling

$$(g_{ds}^Z)_{3\text{-site}} = \frac{e}{2(4\pi)^2 \sin \theta_W \cos \theta_W} \frac{f_1^2 f_2^2}{(f_1^2 + f_2^2)^2} \ln \left(\frac{\Lambda^2}{M^2} \right) \sum_u \frac{V_{ud}^* m_u^2 V_{us}}{v^2} , \quad (64)$$

where we have used Eq. (6) to relate the result to v . The formulae for the other quarks is similar, with the appropriate replacements dictated by the form of $\Delta(\epsilon_L \epsilon_L^\dagger)$ and $\mathcal{M}_{u,d}$.

By comparison, the corresponding standard model result [36] is

$$(g_{ds}^Z)_{SM} = \frac{e}{(4\pi)^2 \sin \theta_W \cos \theta_W} \sum_u \frac{V_{ud}^* m_u^2 A(m_u, M_W) V_{us}}{v^2} , \quad (65)$$

where

$$A(m_u, M_W) = \frac{M_W^2 (2M_W^2 + 3m_u^2)}{(m_u^2 - M_W^2)^2} \log \left(\frac{m_u^2}{M_W^2} \right) + \frac{m_u^2 - 6M_W^2}{m_u^2 - M_W^2} , \quad (66)$$

$$\rightarrow \begin{cases} 1 & m_u \gg M_W \\ 2 \log \frac{m_u^2}{M_W^2} + 6 & m_u \ll M_W . \end{cases} \quad (67)$$

Comparing Eqs. (64) and (65), we see that the new three-site model contributions are, at most, a small fraction of the corresponding (electroweak penguin) standard model result. Since the standard model itself yields Z -penguin amplitudes too small to be unambiguously observed to date, either at the Z -pole or in meson decays, these chiral logarithmic corrections arising from the three-site model are consistent with experiment.

B. $Z' \rightarrow \bar{f}f'$

Next, for completeness, we consider flavor changing couplings of the heavy Z' at one-loop. The form and size of these couplings illustrate the principles of minimal flavor violation and effective field theory we have discussed in the previous section. However, in practice, these couplings are of little phenomenological consequence: because of ideal delocalization, Eq. (56), the only couplings to light fermions are the small hypercharge-related terms in Eq. (50). Therefore, these couplings cannot appreciably contribute to processes such as $B_{s,d} \rightarrow \mu^+ \mu^-$.

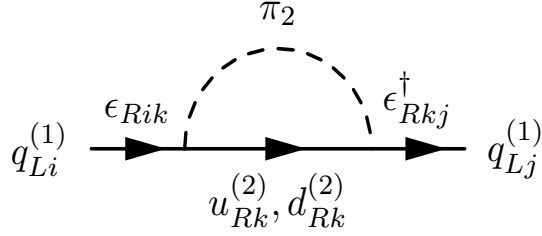


FIG. 4: Wavefunction renormalization that results in the flavor-dependent running of the parameter ϵ_L in the effective theory valid in the energy range below the cutoff scale and above the masses of the heavy fermions. This running yields the renormalization group equation (62). Note that the $q_L^{(1)}$ and $u_R^{(2)}, d_R^{(2)}$ are the site 1 and 2 gauge-eigenstate fermion fields of Eq. (1). In 't-Hooft-Feynman gauge, the leading contribution comes from π_2 , the unphysical Nambu-Goldstone Boson in the non-linear sigma model field Σ_2 of Eq. (2).

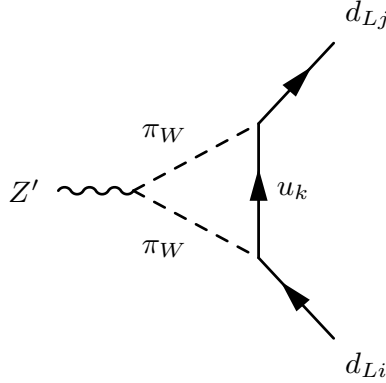


FIG. 5: Z' flavor-changing vertex renormalization arising in the effective theory valid in the energy range below the scale of the heavy fermions M and above the weak boson scale M_W . In 't-Hooft-Feynman gauge the leading contribution comes from the π_W field, the unphysical Goldstone boson eaten by the mass-eigenstate W -boson. The π_W fields couple proportional to the quark masses, as shown in the effective Lagrangian of Eq. (36) and as required by the usual electroweak Ward identities.

Calculating the diagrams shown in Figs. 2 and 3, we find the leading flavor-changing contributions

$$g_{\bar{s}d}^{Z'} = -\frac{\tilde{g}}{2(4\pi)^2} \left(\sum_u \frac{V_{us}^* m_u^2 V_{ud}}{v^2} \right) \left[\frac{v^2}{f_2^2} \log \frac{\Lambda^2}{M^2} + \log \frac{M^2}{m_u^2} \right], \quad (68)$$

where, for illustration, we have considered the $\bar{s}d$ coupling; the generalization to other quark flavors is dictated by the minimal flavor-violating structure. The origin of the two terms in Eq. (68) is rather different. The first term (proportional to $\log(\Lambda^2/M^2)$) exhibits how the running of ϵ_L in Eq. (63) affects the Z' couplings shown in Eq. (51). The second term, as indicated by the presence of $\log(M^2/m_u^2)$, arises in the effective theory between the scale of the heavy fermions (M) and the quark mass (here we assume $m_u = m_t \gg M_W$) in the loop shown in Fig. 5.

In the end, we conclude that there are no phenomenologically significant flavor-changing effects in Z' couplings at this order. As noted above, ideal delocalization eliminates any tree-level flavor-diagonal Z' coupling to light fermions. While the presence of the large coupling \tilde{g} in the one-loop result of Eq. (68) is tantalizing, that enhancement is cancelled in any low-energy process by the suppression from inverse powers of the Z' mass. Hence, there are no appreciable Z' -exchange contribution to $\Delta F = 1$ processes. In principle, Z' -exchange contributions to $\Delta F = 2$ processes are possible – but these are two-loop effects which are substantially smaller than the one-loop standard model “box-diagram” contributions, as we will discuss in Section V.

C. $b \rightarrow s\gamma$

In the subsections above, we have focused on flavor-changing couplings of the Z and Z' bosons. Notably, we saw that the minimal flavor violation of the three-site model implies that the leading new-physics effects are confined to the left-handed sector, just as in the standard model. In contrast, gauge invariance and minimal coupling insure that the chirality preserving couplings of the photon are flavor-diagonal. Instead, the leading operator for the

phenomenologically relevant radiative decay $b \rightarrow s\gamma$ has the form [37]

$$\mathcal{H}_{eff} = -\frac{4G_F A(m_t, M_W)}{\sqrt{2}} V_{ts}^* V_{tb} \left(\frac{e}{16\pi^2} m_b (\bar{s}_L \sigma^{\mu\nu} b_R) F_{\mu\nu} \right), \quad (69)$$

where, to leading order in the standard model [36]

$$A(m_t, M_W) = \frac{3x^3 - 2x^2}{4(x-1)^4} \log x + \frac{-x^3 + 5x^2 + 2x}{8(x-1)^3}; \quad x = \frac{m_t^2}{M_W^2}. \quad (70)$$

New contributions to this process arise in the three-site model from the presence of *right-handed* couplings of the W to b -quarks (see Eq. (52) and [11]), as well as from the presence of new heavy particles in the loop. These contributions have been studied in detail in [30], for the special case $f_1 = f_2 = \sqrt{2}v$. Their results show that the new contributions are only of order 10% of the standard model contribution for the preferred range of $\epsilon_{Rt} < 0.3$ [11], and that including the contributions from the three-site model tends to *improve* the consistency with the experimental results. Varying away from the point $f_1 = f_2$ will increase the masses of the additional particles, decreasing the size of the new three-site corrections. At the very least, the three-site model's prediction for the rate of $b \rightarrow s\gamma$ will be as consistent with experimental data as that of the standard model.

V. $\Delta F = 2$ PROCESSES AT ONE LOOP

In this section, we extend the analysis of the previous section to study the chiral-logarithmically enhanced corrections to $\Delta F = 2$ processes in the three-site model. We show that the combination of minimal flavor violation and ideal fermion delocalization ensures that both the one-loop corrections from $\Delta F = 2$ box diagrams and the two-loop corrections from $\Delta F = 1$ vertices are small compared to similar corrections in the standard model.

The contributions to $\Delta F = 2$ processes in the three-site model are shown in Fig. 6. The contribution from the first diagram corresponds to those in the standard model. Since the couplings of the W in the three-site model agree with their standard model counterparts up to corrections $\mathcal{O}(x^4) \lesssim 10^{-3}$, this diagram essentially reproduces the standard model contribution. In particular, GIM cancellations imply that all contributions involving light fermions are suppressed by *four* powers of the light up-quark masses. Furthermore, because of ideal delocalization, the diagrams shown in Fig. 7 are absent. The absence of the first (upper left-most) diagram insures that there are no new “long-distance” contributions in the three-site model, nor other new contributions depending on light quark masses but not heavy KK quark masses.

Returning to Fig. 6, we recall that \mathbf{M} and \mathbf{m}_1 are flavor-diagonal at tree-level, and that the masses of the heavy KK fermions are approximately degenerate – with deviations proportional to the corresponding light fermion masses [11]. Hence GIM cancellation in the *heavy* fermion sector implies that contributions from the last three diagrams in Fig. 6 are suppressed by $m_q^2/M^2 \lesssim \mathcal{O}(10^{-3})$, where m_q is a mass of a light quark and M is the mass of the KK fermions. To summarize, the combination of ideal delocalization and minimal flavor violation insure that the *new* contributions to $\Delta F = 2$ box diagrams in the three-site model are smaller than or of order *two-loop* corrections to the same $\Delta F = 2$ processes in the standard model – and hence are not phenomenologically excluded.

These points can be illustrated in more detail by considering the leading, chiral-logarithmically enhanced, three-site box diagram contributions, which arise from the second and third diagrams in Fig. 6. These contributions can be described in effective field theory as follows. The rotations defining the left-handed fermion mass eigenstate fields, Eq. (32), are, to leading order, proportional to ϵ_L and therefore flavor-diagonal. The largest flavor non-diagonal

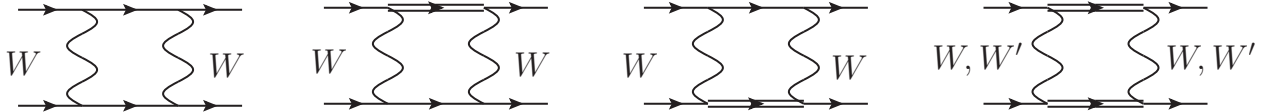


FIG. 6: Diagrams that give dominant contributions to $\Delta F = 2$ processes. The single lines and the double lines represent the standard model and KK fermions, respectively. Because of ideal delocalization, the W' boson does not couple to two light fermions – and therefore only contributes in diagrams involving two heavy intermediate states. The first diagram, including only light standard model states, receives non-standard contributions in the three-site model only to the extent that the weak gauge couplings differ from their standard model equivalents at $\mathcal{O}(x^4)$.

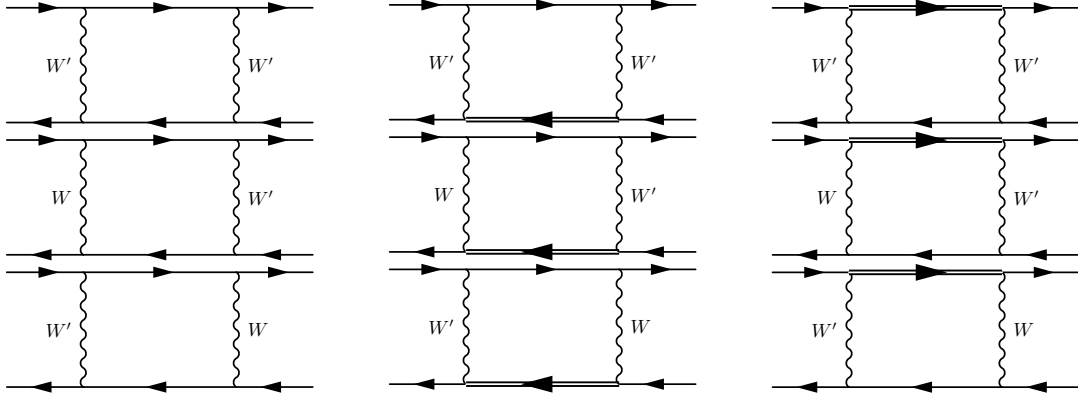


FIG. 7: Diagrams that are absent from the calculation of $\Delta F = 2$ processes in the three-site model, due to ideal delocalization. The single and double lines represent standard model and KK fermions respectively. As described in the text, the combination of ideal delocalization and minimal flavor violation implies that all $\Delta F = 2$ effects are suppressed by $(m/M)^2$, where m and M are the masses of the standard model and KK fermions respectively.

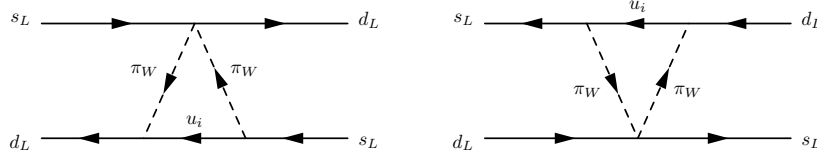


FIG. 8: Diagrams that yield the chiral logarithmically-enhanced three-site model corrections to $\Delta S = 2$ processes in the effective theory, Eq. (36), including the flavor non-universal corrections to ϵ_L shown in Eq. (71). Here π_W are the 't-Hooft-Feynman gauge unphysical Goldstone Bosons eaten by the W boson. As discussed in the text, though enhanced by $\log(M^2/M_W^2)$, all new three-site contributions are even more deeply suppressed by m_q^2/M^2 .

contributions, which can be obtained by diagonalizing $\mathcal{M}^\dagger \mathcal{M}$ to higher order (with \mathcal{M} defined in Eq. (28)), correspond to modifying¹⁰ ϵ_L

$$\Sigma_1 \epsilon_L \rightarrow \Sigma_1 \epsilon_L \cdot \left(\mathcal{I} - M \Sigma_2 \epsilon_R^\dagger \epsilon_R \Sigma_2^\dagger M^{-1} \right). \quad (71)$$

Note that these corrections are consistent with the spurion transformations of Eq. (26). Plugging this correction into the left-handed couplings on the second line of Eq. (36) yields, in 't-Hooft-Feynman gauge, flavor-changing couplings between the left-handed mass-eigenstate quarks and the Goldstone bosons eaten by the W boson. These flavor-changing couplings are proportional to $(\epsilon_L \epsilon_{qR})^2 = (m_q/M)^2$, and the overall result (summing over all intermediate heavy-quark flavors) must include the appropriate CKM mixing matrix elements.

The chiral-logarithmically enhanced three-site box contributions correspond, in the effective theory with heavy KK quarks integrated out, to the diagrams illustrated in Fig. 8 (here shown for $\Delta S = 2$ processes). Viewing these diagrams as a contribution to the effective operator

$$\mathcal{H}_{eff}^{\Delta S=2} = C_K^1 (\bar{s}_L \gamma^\mu d_L) (\bar{s}_L \gamma_\mu d_L), \quad (72)$$

we obtain the leading three-site contribution

$$(C_K^1)_{three-site} = - \frac{\sqrt{2} G_F}{(4\pi)^2} \cdot \frac{v^2}{M^2} \cdot \left(\sum_u \frac{V_{ud}^* m_u^2 V_{us}}{v^2} \right)^2 \cdot \log \frac{M^2}{m_W^2}. \quad (73)$$

¹⁰ There is an analogous shift to ϵ_R proportional to $\epsilon_L^\dagger \epsilon_L$ — however, since ϵ_L is flavor-diagonal at tree-level, these corrections are flavor-universal.

Note that this expression exhibits the specific features described above: (a) suppression by four powers of light fermion masses, (b) as consistent with flavor symmetry, light fermion masses appearing in combination with the usual products of CKM angles, (c) suppression by the heavy KK fermion masses M , and (d) logarithmic enhancement corresponding to “running” from M to the W mass. The generalization¹¹ to other $\Delta F = 2$ processes is straightforward, as determined by flavor symmetry.

Finally, as shown in the previous section, there are no anomalously large $\Delta F = 1$ corrections at the one-loop level in the three-site model – hence, combinations of these $\Delta F = 1$ contributions produce very small $\Delta F = 2$ amplitudes. We conclude that, due to ideal delocalization and minimal flavor violation, there are no large corrections to $\Delta F = 2$ processes in the three-site model.

VI. CONCLUSIONS

In this paper we have explored the flavor structure of the three-site model, and the size of new three-site model contributions to chirality preserving flavor-changing neutral current processes. We established the conditions under which the three-site model exhibits minimal or non-minimal flavor violation, and showed that experimental bounds on flavor-changing effects constrain the tree-level Lagrangian of the three-site model to a form exhibiting only minimal flavor violation.

Assuming minimal flavor violation at the scale of the “cutoff”, *i.e.* the scale of the physics underlying the effective three-site model, we have computed the chiral logarithmic corrections to chirality-preserving flavor-changing neutral current processes. We have shown that the combination of ideal delocalization and minimal flavor violation imply that all flavor-changing $\Delta F = 1$ neutral current processes are parametrically the same size as in the standard model, but numerically smaller. In the case of $\Delta F = 2$ neutral current processes, the combination of ideal delocalization and minimal flavor violation imply that the three-site model contributions are smaller than or of order the two-loop corrections to these processes in the standard model. We conclude, therefore, that the three-site model is phenomenologically consistent with experimental data on (chirality preserving) flavor-changing neutral current processes.

Acknowledgments

RSC and EHS were supported, in part, by the US National Science Foundation under grant PHY-0854889 and also acknowledge the hospitality of the Institute for Advanced Study and the Aspen Center for Physics, where part of this work was completed. M.T.’s work is supported in part by the JSPS Grant-in-Aid for Scientific Research No.20540263 and No.23540298, and he acknowledges the hospitality of the Aspen Center for Physics where part of this work was completed. The figures for this paper were drawn using JaxoDraw [38] and Feynmf [39].

Appendix A: Experimental constraints on the form of ϵ_L

In this Appendix, we establish the experimental constraints on the flavor structure of the charged lepton and quark sectors of the three-site model. We start by calculating the fermion couplings to the weak gauge bosons in a general framework that does not assume ideal fermion delocalization or lepton universality. We then determine the bounds placed on the flavor structure by precision electroweak data and studies of flavor-violating processes. The results demonstrate that the matrices in the tree-level three-site model Lagrangian that govern the delocalization of left-handed quarks (ϵ_L) and left-handed leptons ($\epsilon_{L\ell}$) must be flavor-universal and consistent with ideal fermion delocalization.

1. Electroweak Couplings in the Three-Site Model

In order to compare the electroweak couplings of the fermions in the three-site model with precision electroweak and flavor data, we must first compute the couplings of the fermions to the W - and Z -bosons. Unlike the analysis in

¹¹ There are also other terms that are parametrically smaller (e.g. of order x^4) but numerically similar in size to those discussed here; since they are also small compared to the standard model contributions, including them would not alter our conclusions.

[11], here we will *not* assume ideal delocalization: instead, we will compute the couplings for arbitrary values of the delocalization parameter for the left-handed fermions, ε_L^2 and the ratio

$$x^2 = \frac{g^2}{\tilde{g}^2} \approx \left(\frac{f_1^2 + f_2^2}{v^2} \right) \left(\frac{M_W}{M_{W'}} \right)^2, \quad (\text{A1})$$

In other words, rather than imposing the relation in Eq. (56), we study the degree to which $\epsilon_L \epsilon_L^\dagger$ can deviate from that ideal delocalization value $(\varepsilon_L^{ideal})^2 \cdot \mathcal{I}$.

To investigate the electroweak phenomenology of our model, we display our results in terms of the charge of the electron (14) and the “on-shell” definition of the weak mixing angle [40]:

$$\cos^2 \theta_W = \frac{M_W^2}{M_Z^2}. \quad (\text{A2})$$

Diagonalizing the vector-boson mass matrices, applying the fermion wavefunctions in Eq. (32), and rewriting the results in terms of e and $\sin \theta_W$, we find¹²

$$g_Z = \frac{e}{\sin \theta_W \cos \theta_W} \left[\left(1 - \frac{f_2^2}{f_1^2 + f_2^2} \left\{ \epsilon_L^\dagger \epsilon_L - \frac{x^2 f_1^2}{f_1^2 + f_2^2} \right\} \right) T_3^f - Q^f \sin^2 \theta_W \right], \quad (\text{A3})$$

$$g_W = \frac{e}{\sin \theta_W} \left[1 - \frac{f_2^2}{f_1^2 + f_2^2} \left\{ \epsilon_L^\dagger \epsilon_L - \frac{x^2 f_1^2}{f_1^2 + f_2^2} \right\} \right], \quad (\text{A4})$$

where T_3^f and Q^f are the isospin and charge of fermion species, the couplings are understood to be matrices in flavor space, and these expressions hold up to corrections of $\mathcal{O}(x^4, x^2 \epsilon_L^\dagger \epsilon_L)$. Note that, as advertised, if $\epsilon_L^\dagger \epsilon_L = (\varepsilon_L^{ideal})^2 \cdot \mathcal{I} + \mathcal{O}(x^4)$, the three-site and standard-model predictions agree at tree-level up to this order. Furthermore, the deviation of each coupling from their standard model value is proportional to

$$\delta g_{W,Z} \propto \frac{f_2^2}{f_1^2 + f_2^2} \left\{ \epsilon_L^\dagger \epsilon_L - \frac{x^2 f_1^2}{f_1^2 + f_2^2} \right\} = \left(\frac{M_W}{M_{W'}} \right)^2 \frac{(\epsilon_L^\dagger \epsilon_L - (\varepsilon_L^{ideal})^2 \cdot \mathcal{I})}{(\varepsilon_L^{ideal})^2} \equiv \left(\frac{M_W}{M_{W'}} \right)^2 \frac{\Delta \epsilon_L^\dagger \epsilon_L}{(\varepsilon_L^{ideal})^2}, \quad (\text{A5})$$

where we express the deviation in the delocalization from ideal as a fraction of $(\varepsilon_L^{ideal})^2$ and have used Eqs. (6) and (9) to derive the last expression,

This form of the three-site couplings allows comparison with the LEPWWG [40] extraction of the (flavor-diagonal) fermion couplings to the Z -boson, which (in our notation) assumes the form

$$g_Z^{ff} \equiv \frac{e}{\sin \theta_W \cos \theta_W} \cdot \sqrt{\rho_f} (T_3^f - Q^f \sin^2 \theta_W^{eff}), \quad (\text{A6})$$

where the partial widths and asymmetries for any fermion species are recast as measurements ρ_f and $\sin^2 \theta_{eff}^f$. In the three-site model at tree-level, therefore, we find

$$\sqrt{\rho_f^{3-site}} = 1 - \left(\frac{M_W}{M_{W'}} \right)^2 \frac{[\Delta \epsilon_L^\dagger \epsilon_L]_{ff}}{(\varepsilon_L^{ideal})^2}, \quad (\text{A7})$$

$$\sin^2 \theta_f^{3-site} = \sin^2 \theta_W \left(1 + \left(\frac{M_W}{M_{W'}} \right)^2 \frac{[\Delta \epsilon_L^\dagger \epsilon_L]_{ff}}{(\varepsilon_L^{ideal})^2} \right), \quad (\text{A8})$$

where $[\Delta \epsilon_L^\dagger \epsilon_L]_{ff}$ denotes the appropriate diagonal element of the matrix measuring the deviation of $\epsilon_L^\dagger \epsilon_L$ from ideal.

Finally assuming, for the moment, that $\epsilon_L^\dagger \epsilon_L$ is flavor-universal (proportional to the identity), we may use the techniques of [41] to compute the value of αS from the Z -boson couplings to the T_3 and Y currents

$$g_{3Z} \cdot g_{YZ} = -e^2 \left(1 + \frac{\alpha S}{4 \sin^2 \theta \cos^2 \theta} \right). \quad (\text{A9})$$

¹² These expressions are consistent, to the appropriate order in x^2 , with the form of the $SU(2)$ currents shown in Eq. (54). The form appears different because of the difference between $\sin \theta$, as defined in Eq. (8), and the “on-shell” definition of $\sin \theta_W$.

Applying this to the expression in Eq. (A3), we find

$$\alpha S = -4 \sin^2 \theta_W \left(\frac{M_W}{M_{W'}} \right)^2 \frac{[\Delta \epsilon_L^\dagger \epsilon_L]_{\bar{f}f}}{(\varepsilon_L^{ideal})^2}. \quad (\text{A10})$$

When we study the flavor structure of the quark and lepton sectors, we expect the left-handed delocalization parameter for each flavor to have a value close to $(\varepsilon_L^{ideal})^2$, and we now investigate how large a deviation is allowed by experimental data.

2. The Lepton Sector

We now consider specific experimental constraints on the lepton flavor structure in the three-site model. By analogy with the effective Lagrangian for the quark sector (36), that for the lepton sector of the three-site model may be written, defining $\ell_L \equiv (\nu, \ell^\pm)_L$, as

$$\begin{aligned} \mathcal{L}_{eff} = & \bar{\ell}_L i \not{D} \ell_L + \bar{\ell}_R i \not{D} \ell_R - \left[\bar{\ell}_L \epsilon_{L\ell} \Sigma_1 \Sigma_2 \mathbf{M}_\ell \epsilon_{R\ell} \begin{pmatrix} 0 \\ \ell_R \end{pmatrix} + h.c. \right] \\ & + \bar{\ell}_L \epsilon_{L\ell} \left[\gamma^\mu \Sigma_1 (i D_\mu \Sigma_1^\dagger) \right] \epsilon_{L\ell}^\dagger \ell_L + \bar{\ell}_R \epsilon_{R\ell} \left[\gamma^\mu \Sigma_2^\dagger (i D_\mu \Sigma_2) \right] \epsilon_{R\ell}^\dagger \ell_R, \end{aligned} \quad (\text{A11})$$

where $\epsilon_{L\ell}$ and $\epsilon_{R\ell}$ are defined in parallel with Eqs. (29, 31). We use a basis where the charged lepton mass matrix

$$\mathcal{M}_\ell = \epsilon_{L\ell} \mathbf{M}_\ell \epsilon_{R\ell}^\dagger \quad (\text{A12})$$

in Eq. (A11) is diagonal, and we ignore neutrino masses. We will focus on bounding the elements of the matrix

$$\eta_\ell \equiv \epsilon_{L\ell} \epsilon_{L\ell}^\dagger, \quad (\text{A13})$$

which can induce flavor-dependent Z and Z' couplings to the charged leptons. As discussed above and in [11], we expect the diagonal elements of this matrix to have values close to $(\varepsilon_L^{ideal})^2$ so as to eliminate contributions to αS .

a. Bounds on the diagonal elements of η_ℓ

The LEPWWG analysis [40] of Z boson couplings to charged leptons constrains the diagonal elements of η_ℓ . First, under the assumption of lepton universality, we may bound the amount by which the (presumed identical) diagonal elements $\eta_{\ell ii}$ may differ from $(\varepsilon_L^{ideal})^2$. As mentioned above, the LEPWWG defines a factor ρ_f to accommodate the possibility that physics beyond the standard model shifts the magnitude of the Z boson's coupling to the T_3 charge of fermion f (see Eq. (A6)). Under the assumption of charged lepton universality, they obtain the experimental limit $\rho_\ell = 1.0050 \pm 0.0010$, and give the standard model prediction as $1.00509^{+0.00067}_{-0.00081}$. Because the deviation of $\eta_{\ell ii}$ from the ideal delocalization value is proportional to the departure of ρ_ℓ from its value in the standard model (A7), the LEPWWG bound on ρ_ℓ implies the following 90% CL bound:

$$-0.036 (\varepsilon_L^{ideal})^2 \left(\frac{M_{W'}}{400 \text{ GeV}} \right)^2 < \eta_{\ell ii} - (\varepsilon_L^{ideal})^2 < 0.034 (\varepsilon_L^{ideal})^2 \left(\frac{M_{W'}}{400 \text{ GeV}} \right)^2 \quad (\text{A14})$$

Quantitatively similar results follow from the LEPWWG direct experimental limit on $\sin^2 \theta_\ell^{eff}$ and from measurements of the leptonic asymmetry \mathcal{A}_e . We conclude that, in the case of lepton universality, the diagonal elements of η_ℓ must be within a few percent of $(\varepsilon_L^{ideal})^2$.

Second, we may bound the degree to which the different $\eta_{\ell ii}$ may differ from one another. The LEPWWG has obtained the following bounds on the relative rates at which the Z decays to different flavors of charged leptons [40] :

$$\frac{\Gamma(Z \rightarrow \mu^+ \mu^-)}{\Gamma(Z \rightarrow e^+ e^-)} \equiv \frac{\Gamma_\mu}{\Gamma_e} = 1.0009 \pm 0.0028, \quad \frac{\Gamma(Z \rightarrow \tau^+ \tau^-)}{\Gamma(Z \rightarrow e^+ e^-)} \equiv \frac{\Gamma_\tau}{\Gamma_e} = 1.0019 \pm 0.0032 \quad (\text{A15})$$

and notes that the expected standard model values of these ratios are, respectively, 1.000 and 0.9977. We find that these ratios are directly related to the differences between the various diagonal elements of η_ℓ ; for muons we have (defining $s_\theta \equiv \sin \theta$)

$$\frac{\delta(\Gamma_\mu/\Gamma_e)}{\Gamma_\mu/\Gamma_e} = \frac{\delta\Gamma_\mu}{\Gamma_\mu} - \frac{\delta\Gamma_e}{\Gamma_e} = \frac{(-\frac{1}{2} + s_\theta^2) \left(\frac{f_2^2}{f_1^2 + f_2^2} \right)}{(-\frac{1}{2} + s_\theta^2)^2 + (s_\theta^2)^2} (\eta_{\ell 22} - \eta_{\ell 11}) \quad (\text{A16})$$

and a similar expression holds for taus. The LEPWWG limits on the ratios of partial widths thus yield (at 90% CL)

$$-0.063 (\varepsilon_L^{ideal})^2 \left(\frac{M_{W'}}{400 \text{ GeV}} \right)^2 < \eta_{\ell 22} - \eta_{\ell 11} < 0.043 (\varepsilon_L^{ideal})^2 \left(\frac{M_{W'}}{400 \text{ GeV}} \right)^2, \quad (\text{A17})$$

$$-0.11 (\varepsilon_L^{ideal})^2 \left(\frac{M_{W'}}{400 \text{ GeV}} \right)^2 < \eta_{\ell 33} - \eta_{\ell 11} < 0.012 (\varepsilon_L^{ideal})^2 \left(\frac{M_{W'}}{400 \text{ GeV}} \right)^2. \quad (\text{A18})$$

Using the bounds on the flavor-universal lepton results as indicative of the allowed deviation in the electron couplings and combining the uncertainties in in Eqs. (A17) and (A18) in quadrature with those in Eq. (A14), we find that the bounds:

$$-0.075 (\varepsilon_L^{ideal})^2 \left(\frac{M_{W'}}{400 \text{ GeV}} \right)^2 < \eta_{\ell 22} - (\varepsilon_L^{ideal})^2 < 0.053 (\varepsilon_L^{ideal})^2 \left(\frac{M_{W'}}{400 \text{ GeV}} \right)^2, \quad (\text{A19})$$

$$-0.12 (\varepsilon_L^{ideal})^2 \left(\frac{M_{W'}}{400 \text{ GeV}} \right)^2 < \eta_{\ell 33} - (\varepsilon_L^{ideal})^2 < 0.020 (\varepsilon_L^{ideal})^2 \left(\frac{M_{W'}}{400 \text{ GeV}} \right)^2. \quad (\text{A20})$$

Hence, even without an *a priori* assumption of lepton universality, the diagonal elements of η_ℓ are constrained by the data to nearly equal one another.

b. Bounds on the off-diagonal elements of η_ℓ

We now consider the bounds on the off-diagonal elements $\eta_{\ell ij}$ from lepton-flavor-violating processes. These arise from flavor-changing left-handed neutral-boson couplings contained in the second line of Eq. (A11). Having diagonalized the charged-lepton mass matrix \mathcal{M}_ℓ , the Hermitian flavor matrix η_ℓ in Eq. (A13) is fixed¹³ and, in general, contains off-diagonal elements. In unitary gauge, the gauge-operator in Eq. (A11) becomes

$$\Sigma_1^\dagger (D_\mu \Sigma_1) \rightarrow (g W_{0\mu}^a - \tilde{g} W_{1\mu}^a) \frac{\sigma^a}{2}, \quad (\text{A21})$$

where $g_{0,1}$ and $W_{0,1}$ are the gauge-eigenstate $SU(2)_0 \times SU(2)_1$ fields in the three-site model in Fig. 1. We may re-write the combination of neutral gauge-eigenstate fields into mass-eigenstate fields using Eqs. (17, 18) to find

$$g W_{0\mu}^3 - \tilde{g} W_{1\mu}^3 = \frac{e}{s_\theta c_\theta} \left(\frac{f_2^2}{f_1^2 + f_2^2} \right) Z_\mu - \tilde{g} Z'_\mu, \quad (\text{A22})$$

up to corrections of $\mathcal{O}(x^2)$. Note that the combination $g W_0 - \tilde{g} W_1$ is orthogonal to the photon; therefore, as must be true by charge conservation, there are no flavor-changing electromagnetic couplings.

The flavor-dependent left-handed neutral-boson couplings of the leptons are, then, given by

$$\mathcal{L}_{FCNC} = \pm \frac{1}{2} \cdot \left(\frac{e}{s_\theta c_\theta} \left(\frac{f_2^2}{f_1^2 + f_2^2} \right) Z_\mu - \tilde{g} Z'_\mu \right) \cdot \eta_{\ell ij} \bar{\ell}_{iL}^0 \gamma^\mu \ell_{jL}^0, \quad (\text{A23})$$

Due to suppression proportional to lepton masses, the right-handed flavor-dependent couplings are expected to be small. In contrast to the case of meson-mixing (considered below), in the lepton sector we are interested in low-energy processes arising from only one insertion of the flavor-dependent operators. Hence, only the Z^μ couplings in Eq. (A23) contribute: the Z' couplings to light fermions are suppressed. At low energies, the flavor-dependent Z -boson couplings give rise to the four-fermion operators

$$\mathcal{L}_{FF} = \pm \frac{e^2}{2s_\theta^2 c_\theta^2 M_Z^2} \cdot \left(\frac{f_2^2}{f_1^2 + f_2^2} \right) \eta_{\ell ij} \bar{\ell}_{iL}^0 \gamma_\mu \ell_{jL}^0 \cdot J_Z^\mu + h.c. \quad (\text{A24})$$

$$= 2\sqrt{2} G_F \cdot \eta_{\ell ij} \left(\frac{f_2^2}{f_1^2 + f_2^2} \right) \bar{\ell}_{iL}^0 \gamma_\mu \ell_{jL}^0 \cdot J_Z^\mu + h.c., \quad (\text{A25})$$

¹³ In particular, the matrix η does not change under $SU(3)_{LD} \times SU(3)_{RD}$ transformations.

where $J_Z^\mu = J_3^\mu - Q^\mu \sin^2 \theta$ is the usual current to which the Z -boson couples.

We begin with limits arising from searches for the decay $\mu \rightarrow 3e$, where $BR(\mu^- \rightarrow e^- e^+ e^-) < 1.0 \times 10^{-12}$ at 90% CL [42]. This is easy to scale from ordinary muon decay, where the interaction

$$\mathcal{L}_{\mu\text{-decay}} = 2\sqrt{2}G_F(\bar{\mu}_L\gamma^\mu\nu_{L\mu})(\bar{\nu}_{Le}\gamma^\mu e_L) \quad (\text{A26})$$

yields the width

$$\Gamma(\mu \rightarrow e\nu_\mu\bar{\nu}_e) = \frac{G_F^2 m_\mu^5}{192\pi^3}. \quad (\text{A27})$$

Hence, since $BR(\mu \rightarrow e\nu_\mu\bar{\nu}_e) \simeq 100\%$, from Eq. (A25) we find¹⁴

$$\frac{BR(\mu \rightarrow 3e)}{BR(\mu \rightarrow e\nu_\mu\bar{\nu}_e)} \approx \frac{1}{2} \cdot \left[\eta_{\ell 12} \left(\frac{f_2^2}{f_1^2 + f_2^2} \right) \left(-\frac{1}{2} + \sin^2 \theta \right) \right]^2 < 1.0 \times 10^{-12}. \quad (\text{A28})$$

This yields the bound

$$|\eta_{\ell 12}| < 1.05 \times 10^{-5} \left(\frac{f_1^2 + f_2^2}{2f_2^2} \right) \quad (90\% \text{ CL}) \simeq 1.3 \times 10^{-4} (\varepsilon_L^{\text{ideal}})^2 \left(\frac{M_{W'}}{400 \text{ GeV}} \right)^2. \quad (\text{A29})$$

A quantitatively similar bound on this matrix element is found from data on $\mu Pb \rightarrow e Pb$ conversion.

By similar means, starting from the bound $BR(\tau \rightarrow e\mu\mu) < 2.3 \times 10^{-8}$ at 90% CL, we find

$$\frac{BR(\tau \rightarrow e\mu\mu)}{BR(\tau \rightarrow e\nu_\tau\bar{\nu}_e)} = \left[\eta_{\ell 13} \left(\frac{f_2^2}{f_1^2 + f_2^2} \right) \left(-\frac{1}{2} + \sin^2 \theta \right) \right]^2 < \frac{2.3 \times 10^{-8}}{BR(\tau \rightarrow e\nu_\tau\bar{\nu}_e)}. \quad (\text{A30})$$

Using the fact that $BR(\tau \rightarrow e\nu_\tau\bar{\nu}_e) \simeq 18\%$, we then obtain

$$|\eta_{\ell 13}| < 2.7 \times 10^{-3} \left(\frac{f_1^2 + f_2^2}{2f_2^2} \right) \quad (90\% \text{ CL}) \simeq 3.4 \times 10^{-2} (\varepsilon_L^{\text{ideal}})^2 \left(\frac{M_{W'}}{400 \text{ GeV}} \right)^2. \quad (\text{A31})$$

And, *mutatis, mutandis*, the bound $BR(\tau \rightarrow \mu ee) < 2.7 \times 10^{-8}$ at 90% CL yields

$$|\eta_{\ell 23}| < 2.9 \times 10^{-3} \left(\frac{f_1^2 + f_2^2}{2f_2^2} \right) \quad (90\% \text{ CL}) \simeq 3.6 \times 10^{-2} (\varepsilon_L^{\text{ideal}})^2 \left(\frac{M_{W'}}{400 \text{ GeV}} \right)^2. \quad (\text{A32})$$

c. Lepton Summary

Combining the 90% CL bounds on the lepton flavor structure, therefore we find that the deviations in the elements of the matrix η_ℓ from ideal are bounded by:

$$|\eta_\ell - (\varepsilon_L^{\text{ideal}})^2 \cdot \mathcal{I}| \lesssim (\varepsilon_L^{\text{ideal}})^2 \left(\frac{M_{W'}}{400 \text{ GeV}} \right)^2 \begin{pmatrix} 0.036 & 0.00013 & 0.034 \\ 0.00013 & 0.075 & 0.036 \\ 0.034 & 0.036 & 0.12 \end{pmatrix} \quad (\text{A33})$$

and η_ℓ is therefore essentially constrained to be proportional to the identity, with diagonal elements equal to $(\varepsilon_L^{\text{ideal}})^2$.

3. The Quark Sector

In this section we study the left-handed quark delocalization matrix $\eta = (\epsilon_L^\dagger \epsilon_L)$, introduced in Eq. (59). Using data on flavor-changing neutral currents and Z decays to heavy quarks, we set bounds on the degree to which η can deviate from $(\varepsilon_L^{\text{ideal}})^2 \cdot \mathcal{I}$.

¹⁴ Here the factor of $\frac{1}{2}$ accounts for the identical particles in the $\mu \rightarrow 3e$ final state.

a. Flavor-Changing Neutral Currents

We begin with the most severely constrained interactions: the flavor-changing left-handed neutral-boson couplings contained in the second line of equation (36). Retracing the analysis of lepton-flavor-violation above shows that, at low energies, Z and Z' exchange (see Eq. (A22)) between quarks gives rise to four-fermion operators of the form

$$\mathcal{L}_{L-FCNC} \rightarrow \pm \frac{1}{2!} \cdot \left(\frac{1}{2}\right)^2 \cdot \eta_{ij}\eta_{k\ell} \left[\frac{e^2}{s_\theta^2 c_\theta^2} \left(\frac{f_2^2}{f_1^2 + f_2^2}\right)^2 \frac{1}{M_Z^2} + \frac{\tilde{g}^2}{M_{Z'}^2} \right] (\bar{q}_L^i \gamma^\mu q_L^j) (\bar{q}_L^k \gamma_\mu q_L^\ell), \quad (\text{A34})$$

here the first factor $(1/2!)$ accounts for the two identical currents and the next $((1/2)^2)$ accounts for the T_3 charges of the external fermions. Using the masses of Eq. (9) and the relation in Eq. (6), we find the term in square brackets is approximately $4/f_1^2$ so that

$$\mathcal{L}_{L-FCNC} \rightarrow \pm \frac{\eta_{ij}\eta_{k\ell}}{2f_1^2} (\bar{q}_L^i \gamma^\mu q_L^j) (\bar{q}_L^k \gamma_\mu q_L^\ell). \quad (\text{A35})$$

Ref. [43] has derived constraints on a variety of $\Delta F = 2$ four-fermion operators that cause neutral meson mixing. We will start with their limits on the coefficients (C_j^1) of the operators responsible for mixing in the Kaon, B_d , and B_s systems:

$$C_K^1 (\bar{s}_L \gamma^\mu d_L) (\bar{s}_L \gamma_\mu d_L) \quad C_{B_d}^1 (\bar{b}_L \gamma^\mu d_L) (\bar{b}_L \gamma_\mu d_L) \quad C_{B_s}^1 (\bar{b}_L \gamma^\mu s_L) (\bar{b}_L \gamma_\mu s_L). \quad (\text{A36})$$

The numerical values of the limits they obtain in the down-quark sector in the C_j^1 correspond, in the notation of Eq. (A35), to the constraints

$$-(4.82 \times 10^{-4})^2 < \Re(\eta_{sd})^2 \left(\frac{2v^2}{f_1^2}\right) < (4.82 \times 10^{-4})^2 \quad (\text{A37})$$

$$-(3.26 \times 10^{-5})^2 < \Im(\eta_{sd})^2 \left(\frac{2v^2}{f_1^2}\right) < (2.60 \times 10^{-5})^2 \quad (\text{A38})$$

$$|\eta_{bd}|^2 \left(\frac{2v^2}{f_1^2}\right) < (2.3 \times 10^{-3})^2 \quad (\text{A39})$$

$$|\eta_{bs}|^2 \left(\frac{2v^2}{f_1^2}\right) < (1.63 \times 10^{-2})^2 \quad (\text{A40})$$

or, in a more convenient notation, to

$$|\eta_{ds}| < 4.8 \times 10^{-4} \left(\frac{f_1}{\sqrt{2}v}\right) = 0.0060 (\varepsilon_L^{ideal})^2 \left(\frac{M_{W'}}{400 \text{ GeV}}\right)^2 \left(\frac{\sqrt{2}v}{f_1}\right) \quad (\text{A41})$$

$$|\eta_{bd}| < 2.3 \times 10^{-3} \left(\frac{f_1}{\sqrt{2}v}\right) = 0.0285 (\varepsilon_L^{ideal})^2 \left(\frac{M_{W'}}{400 \text{ GeV}}\right)^2 \left(\frac{\sqrt{2}v}{f_1}\right) \quad (\text{A42})$$

$$|\eta_{bs}| < 1.63 \times 10^{-2} \left(\frac{f_1}{\sqrt{2}v}\right) = 0.202 (\varepsilon_L^{ideal})^2 \left(\frac{M_{W'}}{400 \text{ GeV}}\right)^2 \left(\frac{\sqrt{2}v}{f_1}\right) \quad (\text{A43})$$

In the three-site model, we expect the eigenvalues of the matrix η to be of order $(\varepsilon_L^{ideal})^2$. Hence, with the possible exception of η_{bs} , the data requires that the matrix η be nearly *diagonal* in the down-quark mass-eigenstate basis.

At this point, recalling that $\mathcal{M}_u = V_{CKM}^\dagger \Delta_u$, we also note that there is a low-energy operator that can cause D -meson mixing. This is

$$C_D^1 (\bar{c}_L \gamma^\mu u_L) (\bar{c}_L \gamma_\mu u_L), \quad (\text{A44})$$

with

$$C_D^1 = \pm \frac{1}{2f_1^2} (V_{ud} \eta_{11} V_{cd}^* + V_{us} \eta_{22} V_{cs}^* + V_{ub} \eta_{33} V_{cb}^*)^2, \quad (\text{A45})$$

where the V_{ij} are the elements of the CKM matrix. The authors of [43] report a limit

$$|C_D^1| < 7.2 \times 10^{-13} \text{ GeV}^{-2}, \quad (\text{A46})$$

from which we conclude

$$|V_{ud} \eta_{11} V_{cd}^* + V_{us} \eta_{22} V_{cs}^* + V_{ub} \eta_{33} V_{cb}^*|^2 < (4.17 \times 10^{-4})^2 \left(\frac{f_1^2}{2v^2} \right). \quad (\text{A47})$$

Now, the product of CKM elements appearing in the third term $|V_{ub} V_{cb}^*| \simeq \mathcal{O}(10^{-4})$ is much smaller than those in the other two terms $V_{ud} V_{cd}^* \approx -V_{us} V_{cs}^* \approx .16$. Therefore, barring a very large difference among the diagonal entries of η , we may neglect the η_{33} term in Eq. (A47) and find

$$|\eta_{11} - \eta_{22}| \leq 2.61 \times 10^{-3} \left(\frac{f_1}{\sqrt{2}v} \right) = 0.0323 (\varepsilon_L^{ideal})^2 \left(\frac{M_{W'}}{400 \text{ GeV}} \right)^2 \left(\frac{\sqrt{2}v}{f_1} \right) \quad (\text{A48})$$

Since we anticipate that each of the η_{ii} is of order $(\varepsilon_L^{ideal})^2$, we conclude that $\eta_{11} \approx \eta_{22}$.

This result is consistent with precision electroweak data: η_{11} and η_{22} respectively, determine the delocalization of the first- and second-generation left-handed quarks. Their having different values is disfavored because that would change the relative rates at which the Z decays to up vs. charm or down vs. strange quarks. Similarly, η_{33} controls the delocalization of b_L – and, as discussed below, data on R_b and R_c constrains how much this can differ from $\eta_{11,22}$.

These are the strongest limits available from flavor-changing processes in the quark sector. Bounds on flavor-changing decays in the third generation up-quark sector are rather weak: current limits imply only that $Br(t \rightarrow cZ) < 3.7\%$ [42], which provides no new information on the elements of η . While the B_s or D^0 systems are, respectively, the most promising for eventual limits on right-handed FCNC's in the down and up sectors, no limits presently exist.

b. Z -Pole Constraints on R_b and R_c

The LEPWWG has obtained bounds on the relative rates at which the Z decays to heavy quarks, as compared with decays to all hadrons [40] :

$$\frac{\Gamma(Z \rightarrow b\bar{b})}{\Gamma(Z \rightarrow \text{hadrons})} \equiv R_b = 0.21629 \pm 0.00066 \quad (\text{A49})$$

$$\frac{\Gamma(Z \rightarrow c\bar{c})}{\Gamma(Z \rightarrow \text{hadrons})} \equiv R_c = 0.1721 \pm 0.0030, \quad (\text{A50})$$

and gives the, respective, standard model predictions for these quantities as $0.21583^{+0.00033}_{-0.00045}$ and $0.17225^{+0.00016}_{-0.00012}$. These ratios are useful to work with because QCD corrections, manifesting as dependence on the value of α_s , should largely cancel.¹⁵

Because the data from D-meson mixing has already established that $\eta_{22} = \eta_{11}$, both R_b and R_c may be written as linear combinations of just the two diagonal matrix elements η_{33} and η_{22} :

$$\frac{\delta(R_b)}{R_b} = \frac{\delta\Gamma_b}{\Gamma_b} - \frac{\delta\Gamma_{\text{hadr.}}}{\Gamma_{\text{hadr.}}} = (-0.8924 (\eta_{33} - (\varepsilon_L^{ideal})^2) + 0.0910 (\eta_{22} - (\varepsilon_L^{ideal})^2)) \left[\frac{2f_2^2}{f_1^1 + f_2^2} \right] \quad (\text{A51})$$

$$\frac{\delta(R_c)}{R_c} = \frac{\delta\Gamma_c}{\Gamma_c} - \frac{\delta\Gamma_{\text{hadr.}}}{\Gamma_{\text{hadr.}}} = (0.2512 (\eta_{33} - (\varepsilon_L^{ideal})^2) + 1.297 (\eta_{22} - (\varepsilon_L^{ideal})^2)) \left[\frac{2f_2^2}{f_1^1 + f_2^2} \right], \quad (\text{A52})$$

Solving the coupled equations for the two $\eta_{ii} - (\varepsilon_L^{ideal})^2$ yields the limits

$$-0.093 (\varepsilon_L^{ideal})^2 \left(\frac{M_{W'}}{400 \text{ GeV}} \right)^2 < \eta_{33} - (\varepsilon_L^{ideal})^2 < 0.020 (\varepsilon_L^{ideal})^2 \left(\frac{M_{W'}}{400 \text{ GeV}} \right)^2, \quad (\text{A53})$$

$$-0.30 (\varepsilon_L^{ideal})^2 \left(\frac{M_{W'}}{400 \text{ GeV}} \right)^2 < \eta_{22} - (\varepsilon_L^{ideal})^2 < 0.30 (\varepsilon_L^{ideal})^2 \left(\frac{M_{W'}}{400 \text{ GeV}} \right)^2. \quad (\text{A54})$$

¹⁵ In principle, one could try to extract limits on η_{33} from the product $R_b R_c$, because the fractional change would depend only on η_{33} and $\eta_{\ell ii}$, and the latter is already tightly constrained to have the value $(\varepsilon_L^{ideal})^2$. However, the usefulness of this approach is limited by the fact that the standard model prediction of R_ℓ is subject to significant uncertainty through its dependence on α_s .

while rotating (A51) and (A52) into the $\eta_{33} \pm \eta_{22}$ basis says, equivalently:

$$-0.48 (\varepsilon_L^{ideal})^2 \left(\frac{M_{W'}}{400 \text{ GeV}} \right)^2 < \eta_{33} - \eta_{22} < 0.41 (\varepsilon_L^{ideal})^2 \left(\frac{M_{W'}}{400 \text{ GeV}} \right)^2. \quad (\text{A55})$$

We conclude that η_{33} is constrained at 90% CL to lie within a few percent of the ideal delocalization value, while η_{22} (and η_{11}) must lie within about 30% of the ideal delocalization value and within about 45% of η_{33} . The limit on η_{22} is consistent with what the LEPWWG data on ρ_c implies; the limit on η_{33} surpasses that obtained from ρ_b .

c. Summary

Combining the 90% CL bounds for the η_{ii} obtained in this section, we find that deviations in the elements of the matrix η from ideal delocalization are bounded by:

$$|\eta - (\varepsilon_L^{ideal})^2 \cdot \mathcal{I}| \lesssim (\varepsilon_L^{ideal})^2 \left(\frac{M_{W'}}{400 \text{ GeV}} \right)^2 \begin{pmatrix} 0.30 & 0.0060 \frac{\sqrt{2}v}{f_1} & 0.0285 \frac{\sqrt{2}v}{f_1} \\ 0.0060 \frac{\sqrt{2}v}{f_1} & 0.30 & 0.202 \frac{\sqrt{2}v}{f_1} \\ 0.0285 \frac{\sqrt{2}v}{f_1} & 0.202 \frac{\sqrt{2}v}{f_1} & 0.09 \end{pmatrix}, \quad (\text{A56})$$

subject to the constraints on $\eta_{22} - \eta_{11}$ and $\eta_{33} - \eta_{22}$ noted above. The factors of $\sqrt{2}v/f_1$ in the off-diagonal elements reflect the fact that those bounds arise from joint Z and Z' contributions to $\Delta F = 2$ meson mixing processes; the constraints on the diagonal elements, like all the elements of η_ℓ , come from decay processes involving only Z couplings. We conclude that the flavor matrix η for quarks must be nearly proportional to the identity matrix.

-
- [1] C. Csaki, *et. al.*, Phys. Rev. D **69**, 055006 (2004) [arXiv:hep-ph/0305237].
 - [2] S. Weinberg, Phys. Rev. D **19**, 1277 (1979).
 - [3] L. Susskind, Phys. Rev. D **20**, 2619 (1979).
 - [4] G. Cacciapaglia, C. Csaki, C. Grojean and J. Terning, Phys. Rev. D **71** (2005) 035015 [arXiv:hep-ph/0409126].
 - [5] R. Casalbuoni, S. De Curtis, D. Dolce and D. Dominici, Phys. Rev. D **71**, 075015 (2005) [arXiv:hep-ph/0502209].
 - [6] G. Cacciapaglia, C. Csaki, C. Grojean, M. Reece and J. Terning, Phys. Rev. D **72**, (2005) 095018 [arXiv:hep-ph/0505001].
 - [7] R. Foadi, S. Gopalakrishna and C. Schmidt, Phys. Lett. B **606** (2005) 157 [arXiv:hep-ph/0409266].
 - [8] R. Foadi and C. Schmidt, Phys. Rev. D **73** (2006) 075011 [arXiv:hep-ph/0509071].
 - [9] R. S. Chivukula, E. H. Simmons, H. J. He, M. Kurachi and M. Tanabashi, Phys. Rev. D **71**, 115001 (2005) [arXiv:hep-ph/0502162].
 - [10] R. Sekhar Chivukula, E. H. Simmons, H. J. He, M. Kurachi and M. Tanabashi, Phys. Rev. D **72**, 015008 (2005) [arXiv:hep-ph/0504114].
 - [11] R. Sekhar Chivukula, B. Coleppa, S. Di Chiara, E. H. Simmons, H. J. He, M. Kurachi and M. Tanabashi, Phys. Rev. D **74**, 075011 (2006) [arXiv:hep-ph/0607124].
 - [12] T. Abe, S. Matsuzaki and M. Tanabashi, Phys. Rev. D **78**, 055020 (2008) [arXiv:0807.2298 [hep-ph]].
 - [13] R. Casalbuoni, S. De Curtis, D. Dominici, and R. Gatto, Phys. Lett. **B155**, 95 (1985).
 - [14] R. Casalbuoni *et. al.*, Phys. Rev. **D53**, 5201 (1996).
 - [15] M. Bando, T. Kugo, S. Uehara, K. Yamawaki, and T. Yanagida, Phys. Rev. Lett. **54**, 1215 (1985).
 - [16] M. Bando, T. Kugo, and K. Yamawaki, Nucl. Phys. **B259** 493 (1985).
 - [17] M. Bando, T. Fujiwara, and K. Yamawaki, Prog. Theor. Phys. **79**, 1140 (1988).
 - [18] M. Bando, T. Kugo, and K. Yamawaki, Phys. Rept. **164** (1988), 217 (1988).
 - [19] M. Harada and K. Yamawaki, Phys. Rept. **381**, 1 (2003).
 - [20] R. S. Chivukula and H. Georgi, Phys. Lett. B **188**, 99 (1987).
 - [21] G. D'Ambrosio, G. F. Giudice, G. Isidori and A. Strumia, Nucl. Phys. B **645**, 155 (2002) [arXiv:hep-ph/0207036].
 - [22] M. E. Peskin and T. Takeuchi, Phys. Rev. Lett. **65**, 964 (1990).
 - [23] M. E. Peskin and T. Takeuchi, Phys. Rev. D **46**, 381 (1992).
 - [24] G. Altarelli and R. Barbieri, Phys. Lett. B **253**, 161 (1991).
 - [25] G. Altarelli, R. Barbieri and S. Jadach, Nucl. Phys. B **369**, 3 (1992) [Erratum-ibid. B **376**, 444 (1992)].
 - [26] S. Matsuzaki, R. S. Chivukula, E. H. Simmons and M. Tanabashi, Phys. Rev. D **75**, 073002 (2007) [arXiv:hep-ph/0607191].
 - [27] R. S. Chivukula, E. H. Simmons, S. Matsuzaki and M. Tanabashi, Phys. Rev. D **75**, 075012 (2007) [arXiv:hep-ph/0702218].
 - [28] S. Dawson and C. B. Jackson, Phys. Rev. D **76**, 015014 (2007) [arXiv:hep-ph/0703299].
 - [29] T. Abe, R. S. Chivukula, N. D. Christensen, K. Hsieh, S. Matsuzaki, E. H. Simmons, M. Tanabashi, Phys. Rev. **D79**, 075016 (2009). [arXiv:0902.3910 [hep-ph]].
 - [30] M. Kurachi, T. Onogi, Prog. Theor. Phys. **125** (2011) 103-128. [arXiv:1006.3414 [hep-ph]].

- [31] H. Georgi, Nucl. Phys. **B266**, 274 (1986).
- [32] T. Appelquist, J. Carazzone, Phys. Rev. **D11**, 2856 (1975).
- [33] S. L. Glashow, J. Iliopoulos and L. Maiani, Phys. Rev. D **2** (1970) 1285.
- [34] N. Cabibbo, Phys. Rev. Lett. **10** (1963) 531.
- [35] M. Kobayashi and T. Maskawa, Prog. Theor. Phys. **49**, 652 (1973).
- [36] T. Inami, C. S. Lim, Prog. Theor. Phys. **65**, 297 (1981).
- [37] B. Grinstein, R. P. Springer, M. B. Wise, Phys. Lett. **B202**, 138 (1988).
- [38] D. Binosi and L. Theussl, Comput. Phys. Commun. **161**, 76 (2004) [arXiv:hep-ph/0309015].
- [39] T. Ohl, Comput. Phys. Commun. **90**, 340-354 (1995). [hep-ph/9505351].
- [40] [ALEPH Collaboration and DELPHI Collaboration and L3 Collaboration and], Phys. Rept. **427**, 257 (2006) [arXiv:hep-ex/0509008].
- [41] R. S. Chivukula, E. H. Simmons, H. J. He, M. Kurachi and M. Tanabashi, Phys. Rev. D **70**, 075008 (2004) [arXiv:hep-ph/0406077].
- [42] C. Amsler *et al.* [Particle Data Group], Phys. Lett. B **667**, 1 (2008).
- [43] M. Bona *et al.* [UTfit Collaboration], JHEP **0803**, 049 (2008) [arXiv:0707.0636 [hep-ph]].